CP-63883
Revision 0

Vadose Zone Flow and Transport Parameters Data Package for the Hanford Site Composite Analysis

Prepared for the U.S. Department of Energy
Assistant Secretary for Environmental Management

Contractor for the U.S. Department of Energy
under Contract DE-AC06-08RL14788

CH2MHILL
Plateau Remediation Company

P.O. Box 1600
Richland, Washington 99352

CP-63883
Revision 0

Vadose Zone Flow and Transport Parameters Data Package for the Hanford Site Composite Analysis

Document Type: DP Program/Project: EP&SP

R. Khaleel
INTERA, Inc.

Date Published
April 2020

Prepared for the U.S. Department of Energy
Assistant Secretary for Environmental Management

Contractor for the U.S. Department of Energy
under Contract DE-AC06-08RL14788

CH2MHILL
Plateau Remediation Company
P.O. Box 1600
Richland, Washington 99352

APPROVED
By Sarah Harrison at 7:26 am, Apr 07, 2020

Release Approval Date

Printed in the United States of America

Executive Summary

This report provides a description of the basis for the development and implementation of a conceptual model for vadose zone flow and transport for the Hanford Site composite analysis (CA) groundwater pathway analysis. The parameterization for a numerical model is intimately linked to the conceptual model framework. This report describes the basis for the selection of hydraulic and transport parameters for the hydrostratigraphic units (HSUs) identified in the 200 East and 200 West Areas. The following three-step process was used to develop the hydraulic properties and transport parameters for the CA modeling:

1. **Breakdown** of existing database on hydraulic properties by HSUs
2. **Constitutive model** parameters for laboratory, core-scale hydraulic properties
3. **Upscaling** for macroscopic, field-scale flow, and transport parameters

This document provides data and information on the following items:

- A brief description and technical basis for the conceptual model selected to represent vadose zone flow and transport for the CA modeling
- Variation in sediment particle size distribution for representative sites in the 200 East and West Areas
- A summary of effective (upscaled) moisture retention, and saturated and unsaturated hydraulic conductivity estimates for the HSUs in the 200 East and West Areas
- A summary of effective transport parameters, including sediment bulk density and macrodispersivity estimates for various HSUs
- The 200 East Area B Complex perched water aquifer hydraulic properties

This page intentionally left blank.

Contents

Figures

Tables

This page intentionally left blank.

Terms

3D	three-dimensional
CA	composite analysis
CCU	Cold Creek unit
CCUc	Cold Creek unit caliche
CCUg	Cold Creek unit gravel
CCUz	Cold Creek unit silt
EHM	equivalent homogeneous medium
eSTOMP	multi-processor capable extreme-scale STOMP
Hf1	Hanford formation unit 1
Hf2	Hanford formation unit 2
Hf3	Hanford formation unit 3
HSU	hydrostratigraphic unit
IDF	Integrated Disposal Facility
MDA	moisture-dependent anisotropy
MRC	moisture retention curve
PA	power-averaging
PA-TCT	power-averaging and tensorial connectivity-tortuosity
PSD	particle size distribution
PWA	perched water aquifer
ROCSAN	ROCkwell Hanford Operations Sediment Analysis
Rtf	Ringold Formation member of Taylor Flat
Rwia	Ringold Formation member of Wooded Island – unit A
Rwie	Ringold Formation member of Wooded Island – unit E
S&L	Sisson and Lu
STOMP	Subsurface Transport Over Multiple Phases
TCT	tensorial-connectivity tortuosity

This page intentionally left blank.

1 Introduction

This report provides a description of the basis for the development and implementation of a conceptual model for vadose zone flow and transport for the composite analysis (CA) groundwater pathway analysis. The parameterization for a numerical model is intimately linked to the conceptual model framework. The report describes the basis for the selection of hydraulic and transport parameters for the hydrostratigraphic units (HSUs) identified in the 200 East and 200 West Areas. Whenever data are sparse or unavailable, surrogate hydraulic properties are chosen based on samples collected within the 200 Areas and nearby locations that are representative of sediments characteristic of the HSUs identified elsewhere.

The following information is included in this report:

- A brief description and technical basis for the conceptual model selected to represent vadose zone flow and transport for the CA modeling
- Variation in sediment particle size distribution (PSD) for representative sites in the 200 East and West Areas
- A summary of effective (upscaled) moisture retention, and saturated and unsaturated hydraulic conductivity estimates for the HSUs in the 200 East and West Areas
- A summary of effective transport parameters including macrodispersivity estimates for various HSUs
- The 200 East Area B Complex perched water aquifer hydraulic properties

2 Flow and Transport Modeling Approaches

Within the 200 Areas of the Hanford Site, vadose zone sediments are heterogeneous at a variety of scales. For example, an outcrop (Figure 1) provides an illustrative example of the inherent variability in geologic media that can be observed in vadose zone sediments. Depending on the resolution needed in a modeling analysis, a variety of conceptual models can be developed and implemented to approximate flow through this example outcrop encompassing heterogeneous media. With respect to predictive resolution, however, geologic conceptual models can be classified into two broad categories: an equivalent homogeneous medium (EHM) model and a heterogeneous media model.

Following the EHM modeling approach, the outcrop in Figure 1, for instance, may be mapped into three distinct large-scale geologic formations based on facies distribution (Figure 2, inset a). Each HSU is then assumed to have representative, but uniform values in terms of vadose zone hydraulic properties (Figure 2, inset a). Each HSU is, however, treated as an anisotropic EHM. As discussed below, the equivalent homogeneous conceptual modeling approach uses small-scale laboratory measurements to predict the large, field-scale flow behavior. On the contrary, Figure 2 inset b, in effect, conceptualizes the heterogeneous geologic media as a collection of numerous small blocks with different hydraulic properties, mimicking the detailed spatial variability that is inherent in geologic deposits. The EHM modeling is the preferred approach for the CA flow and transport modeling.

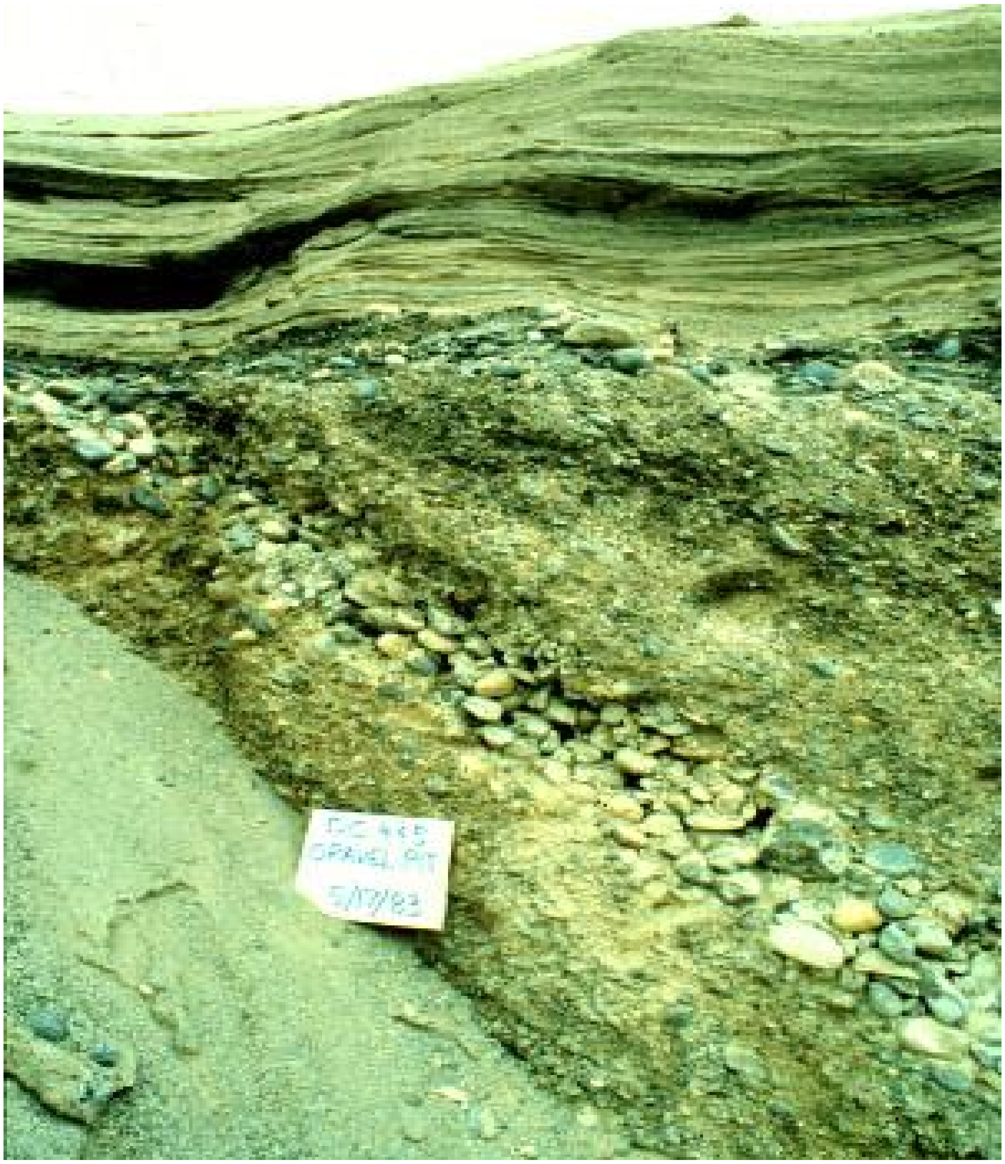

Source: Yeh et al., 2015, *Flow Through Heterogeneous Geologic Media*.

Figure 1. Heterogeneous Geologic Outcrop in the 200 East Area

(inset a)

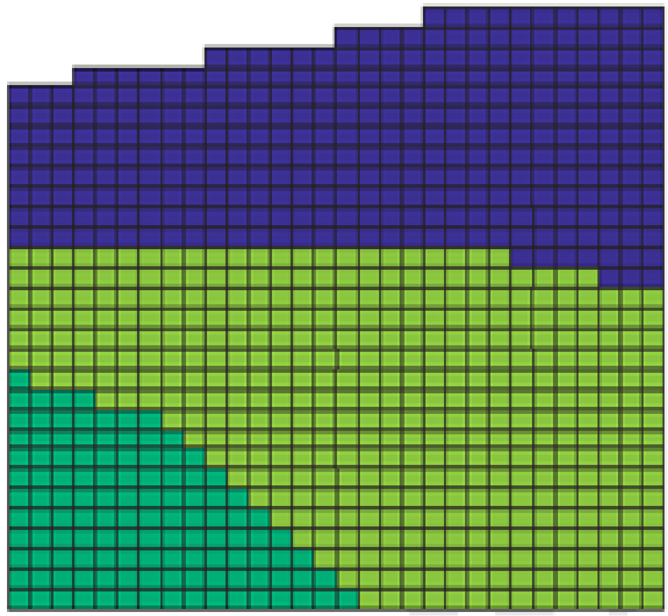

(inset b)

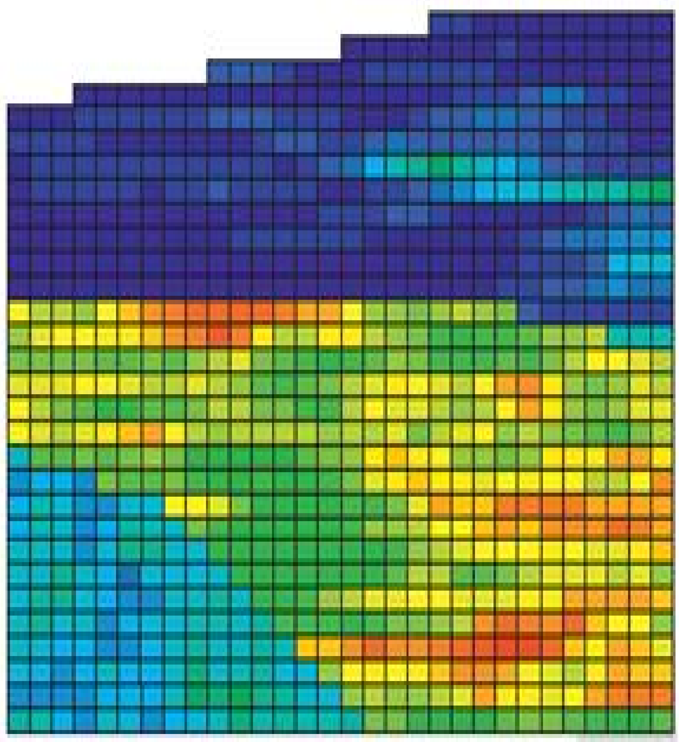

Note: (a) an anisotropic equivalent homogeneous medium representation with each unit having its own uniform average properties, and (b) different hydraulic properties for each grid block in the model grid representing the outcrop (adapted from Yeh et al., 2015, *Flow Through Heterogeneous Geologic Media*).

Figure 2. Modeling Approaches for a Heterogeneous Geologic Outcrop

3 Flow and Transport Codes

The selected flow and transport codes for the CA numerical simulations are the Subsurface Transport Over Multiple Phases (STOMP)[1] simulator and the multi-processor capable extreme-scale STOMP (eSTOMP) simulator. These codes allow for the numerical translation of the vadose zone conceptual model for flow and transport.

STOMP and eSTOMP solve the Richards' equation (the water mass conservation equation described in PNNL-12030, *STOMP Subsurface Transport Over Multiple Phases Version 2.0 Theory Guide*) and the advection-dispersion equation (the solute mass conservation equation described in PNNL-12030) that govern the water flow and solute transport, respectively, under variably saturated conditions in the vadose zone and saturated media.

STOMP and eSTOMP have been selected because these codes fulfill the required features and specifications described below. There is an extensive history of application of STOMP at the Hanford Site and elsewhere including verification, benchmarking, and data comparisons.

4 Constitutive Relations for Sediment Hydraulic Properties

Several parameters are needed to model the vadose zone flow and contaminant transport. Among the hydrologic data, constitutive relations for hydraulic properties (i.e., soil moisture content versus matric potential and unsaturated hydraulic conductivity versus matric potential or moisture content relationships) are key to quantifying the moisture storage and flow properties of vadose zone sediments. The same constitutive relations are used for EHM as well as heterogeneous media models. The soil moisture content versus matric potential relationships are described for each HSU (for EHM model) or grid block (for heterogeneous model) using the empirical relationship (van Genuchten, 1980, "A Closed-Form Equation for Predicting the Hydraulic Conductivity of Unsaturated Soils") shown in Equation 1:

$$\theta(h) = \theta_r + (\theta_s - \theta_r)\{1 + [\alpha h]^n\}^{-m} \qquad \textbf{(Eq. 1)}$$

where:

$\theta(h)$	=	the moisture content expressed explicitly as a function of the soil matric potential h
θ_r	=	residual moisture content (dimensionless)
θ_s	=	saturated moisture content (dimensionless)
α	=	a fitting parameter (L^{-1})
n	=	a fitting parameter (dimensionless)
m	=	$1 - 1/n$.

Combining the van Genuchten model with Mualem's (1976) model ("A New Model for Predicting the Hydraulic Conductivity of Unsaturated Porous Media") produces the following relationship for unsaturated hydraulic conductivity, K:

$$K(S_e) = K_s S_e^l \left\{1 - \left(1 - S_e^{(1/m)}\right)^m\right\}^2 \qquad \textbf{(Eq. 2)}$$

[1] Battelle Memorial Institute retains the copyright on all versions, revisions, and operational modes of the Subsurface Transport Over Multiple Phases (STOMP) software simulator as permitted by the U.S. Department of Energy. STOMP is included here under a limited government use license.

where:

S_e = effective saturation = $(\theta-\theta_r)/(\theta_s-\theta_r)$

K_s = the saturated hydraulic conductivity (cm/s)

l = pore-connectivity parameter (dimensionless).

Mualem (1976) estimated l as being about 0.5, an average of 45 samples. For the CA, l is treated as being directional, and pore-interaction terms l_{xx}, l_{yy}, and l_{zz} are defined to characterize the large, field-scale variable, moisture-dependent anisotropy (MDA) invoked as part of EHM modeling. While other constitutive relations are available and programmed in STOMP and eSTOMP, the van Genuchten-Mualem formulation is used because of the existence of an extensive database for Hanford Site sediments using this particular formulation (WHC-EP-0883, *Variability and Scaling of Hydraulic Properties for 200 Area Soils, Hanford Site*).

5 Equivalent Homogeneous Medium Modeling

This chapter provides discussions on the following topics:

- EHM modeling essentials
- Upscaling and MDA
- Variable anisotropy model
- Testing and evaluation of the variable anisotropy model

5.1 Equivalent Homogeneous Medium Modeling Essentials

Unlike a heterogeneous media model (Figure 2, inset b) wherein each STOMP grid has variable hydraulic properties relative to moisture retention and unsaturated conductivity, it is not readily apparent as to how the spatial variability of hydraulic properties is embedded in an EHM model (Figure 2, inset a). The following discussion is an attempt in presenting the basics of EHM modeling and how an EHM model is populated.

Stochastic characterization of the spatial variability of flow and transport properties has been found to be an effective method to treat subsurface heterogeneity and to represent upscaled flow and transport properties at the field scale (Dagan, 1989, *Flow and Transport in Porous Formations*; Gelhar, 1993, *Stochastic Subsurface Hydrology*; National Research Council, 2001, *Science and Technology for Environmental Cleanup at Hanford*; Yeh et al., 2015, *Flow Through Heterogeneous Geologic Media*). Following stochastic theory, the goal is then to develop relationships expressing the pressure head variations in terms of the *mean* pressure head field, which yields the *mean* stochastic equation describing the large, field-scale behavior. This is advantageous since the *ensemble mean* form of the governing equations (i.e., Richards' equation and advective dispersive equation) solved by STOMP have the same form as those of the laboratory-scale problem, implying that the laboratory-scale equations can be upscaled for field-scale problems.

For the heterogeneous media, the small-scale laboratory measurements on hydraulic properties are used to simulate the large field-scale behavior. Each heterogeneous geologic unit is replaced by an EHM with upscaled or effective (macroscopic) flow properties. The upscaling process, in addition to being a practical tool given the sparse supporting database for modeling, honors the underlying flow dynamics. For example, the upscaled or effective hydraulic conductivity is the hydraulic conductivity of an EHM (Figure 2, inset a) that produces the same Darcian flux as with the stratified, layered media (Figure 1) under the same boundary conditions. Similarly, the composite soil moisture retention curve (MRC) for an

EHM is the upscaled (effective) MRC based on the laboratory measured retention data of sediment samples. Details on how the EHM modeling domains for different Hanford Site HSUs are populated, based on laboratory-measured hydraulic properties data, are described in Section 1.6.

Because of geologic heterogeneity (and the resulting variability in state variables and macroscopic unsaturated hydraulic conductivity), a variable MDA is prevalent in the field. Such an MDA in the effective unsaturated hydraulic conductivity for an EHM model for the stratified Hanford Site sediments yields greater spreading in the lateral directions than in the vertical direction. It should be emphasized, however, that the effective hydraulic conductivity macroscopic anisotropy results from the volume averaging over a control volume of heterogeneities at a multiplicity of scales (i.e., it is a product of the upscaling process). In fact, the concept of such a large-scale anisotropy is unnecessary, if the multiscale heterogeneities of a geologic formation can be depicted in sufficient detail at a relatively fine-scale resolution consistent with that of laboratory core samples (Figure 2, inset b). Nonetheless, as the length scale transitions from the pore- to core- to field-scale, spatial variability of properties for various HSUs, is believed to dominate the STOMP grid-scale variability.

The development of EHM to approximate the spatially variable parameters of the heterogeneous HSUs involves use of the ergodic hypothesis, which is implicit in the stochastic approach. A stochastic process is said to be ergodic if its statistical properties can be deduced from a single, sufficiently long, random sample of the process. The inclusion of the ergodic hypothesis implies that all possible states existing in the ensemble will be encountered in a single realization of the heterogeneous media if the spatial domain is sufficiently large. The application of the ergodic hypothesis involves exchanging the spatial average of a stochastic variable for the average of the ensemble of realizations of the variable. Thus, for heterogeneous media, the statistics of the ensemble can be determined from a given realization by spatial averaging, and the two averages, spatial and ensemble, can be interchanged (Yeh et al., 2015). The EHM model represents the expected values in the context of ensemble averaging over numerous realizations. The EHM model does not capture the distinct variation in the field data (i.e., a single realization), because the EHM model is based on the ensemble averaging of multiple realizations. However, the EHM model does honor the mean or the bulk flow behavior (Zhang and Khaleel, 2010, “Simulating Field-Scale Moisture Flow Using a Combined Power-Averaging and Tensorial Connectivity-Tortuosity Approach”; Yeh et al., 2005, “Estimation of Effective Unsaturated Hydraulic Conductivity Tensor Using Spatial Moments of Observed Moisture Plume”).

5.2 Upscaling and Moisture-Dependent Anisotropy

Earlier work in hydrology literature treated anisotropy of unsaturated hydraulic conductivity as an intrinsic property, the same as the anisotropy in saturated hydraulic conductivity. Thus, the unsaturated hydraulic conductivity anisotropy has often been modeled by scaling the unsaturated hydraulic conductivity versus the pressure head relationship in different directions as in saturated media. The anisotropy thus remains constant over the full range of saturation or pressure head (i.e., a constant anisotropy concept). However, such a simplistic approach is inappropriate due to the presence of highly nonlinear relationship that is prevalent between the unsaturated hydraulic conductivity and the pressure head or matric potential.

Following stochastic theory (Yeh et al., 1985, “Stochastic Analysis of Unsaturated Flow in Heterogeneous Soils, 2. Statistically Anisotropic Media with Variable α”), the field-scale macroscopic anisotropy of the effective unsaturated hydraulic conductivity for an EHM varies with the mean pressure head or the mean moisture content. This phenomenon is referred to as MDA or pressure head-dependent anisotropy (Yeh et al., 1985). That is, the macroscopic anisotropy (ratio of the effective unsaturated conductivity parallel to geologic bedding to the unsaturated conductivity perpendicular to bedding) increases as the medium becomes less saturated. Such a unique behavior provides explanation for the ubiquitous lateral spreading of observed moisture plumes in the stratified sediments (Yeh et al., 2005).

An illustrative sketch of the pressure head distribution during an infiltration event in a stratified heterogeneous media is shown in Figure 3. Near the infiltration source where the degree of saturation is high, the pressure head contour is generally smooth and symmetrical (dark blue contour). Away from the infiltration source, the pressure head contours (light green and yellow contours) become more irregular and asymmetrical (i.e., large variability). Overall, the pressure head distributions spread out to greater distances horizontally because of media heterogeneities.

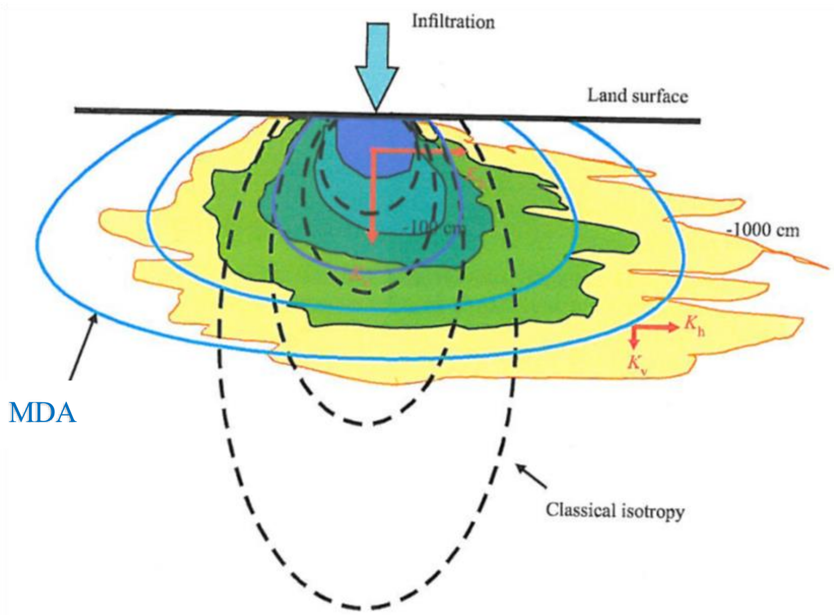

Source: Yeh et al., 2015, "Flow Through Heterogeneous Geologic Media."

Note: The lengths of the red arrows denote the magnitudes of unsaturated hydraulic conductivity in the horizontal direction (K_h) and in the vertical direction (K_v) at the pressure head of the given location.

Figure 3. Schematic Illustrating Pressure Head Distributions During an Infiltration Experiment to Explain Moisture-Dependent Anisotropy (blue curves)

Figure 3 shows the pressure head distributions (black dashed lines) for an equivalent homogeneous and isotropic conceptual model. These lines are smooth and symmetrical, and are elongated in the vertical direction, reflecting effects of gravity and hydraulic conductivity isotropy. Nonetheless, this homogeneous and isotropic conceptual model apparently overestimates the vertical migration and underestimates the lateral spreading of the actual moisture plume in the field.

The blue solid lines (Figure 3) are the simulated pressure head distributions for an EHM model with MDA. That is, the hydraulic conductivity values in the horizontal and the vertical direction are almost the same near the infiltration source where the sediments are wet. In the region where the sediments are dry, both the horizontal and vertical hydraulic conductivities are smaller than those in the wet region, but the ratio of the horizontal hydraulic conductivity to the vertical is much greater than this ratio in the wet region (Figure 3). As stated earlier, such an MDA (Figure 3) in the effective unsaturated hydraulic conductivity for an EHM model for the stratified sediments yields greater spreading in the lateral directions than in the vertical direction. Figure 4 illustrates aspects of a constant and variable macroscopic anisotropy.

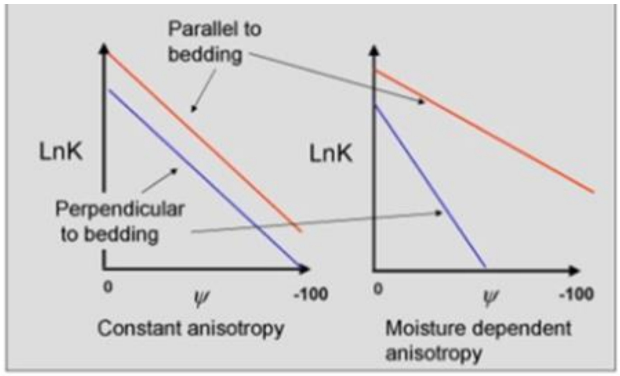

Note: ψ is the matric potential and LnK is the natural logarithm of unsaturated hydraulic conductivity.

Figure 4. Schematic Illustrating Aspects of a Constant (left) and Variable (right) Macroscopic Anisotropy

5.3 Variable Anisotropy Model

Based on the preceding discussion, moisture or tension-dependent anisotropy provides a framework for upscaling small-scale measurements to the effective (upscaled) properties for the large-scale, macroscopic vadose zone (Figure 1). A tensorial connectivity-tortuosity (TCT) model (Zhang et al., 2003, "A Tensorial Connectivity–Tortuosity Concept to Describe the Unsaturated Hydraulic Properties of Anisotropic Soils") is used to evaluate and apply moisture (tension) dependent anisotropy. Details about the development of the MDA model and its application are presented in PNNL-23711, *Physical, Hydraulic, and Transport Properties of Sediments and Engineered Materials Associated with Hanford Immobilized Low-Activity Waste*.

A stochastic model (Polmann, 1990, "Application of Stochastic Methods to Transient Flow and Transport in Heterogeneous Unsaturated Soils") can also be invoked to model MDA and develop the upscaled (effective) parameter estimates. Both Polmann and TCT models serve the same purpose, and both models are coded in STOMP. Unlike the Polmann model, the TCT model has the advantage that its data requirements are much less stringent and has unrestricted application over the entire range of saturation from dry to wet. Furthermore, an evaluation of the TCT model using a controlled database has been performed and is discussed later.

Zhang and Khaleel (2010) developed a practical approach to estimate the three-dimensional (3D) effective unsaturated hydraulic conductivity via a combined power-averaging and tensorial connectivity-tortuosity (PA-TCT) model. With the power-averaging (PA) model, for each stratigraphic unit, the effective unsaturated hydraulic conductivity in the i^{th} principal direction, $K_i^e(h)$, for an anisotropic EHM, as a function of pressure head h, was estimated as

$$K_i^e(h) = \left\{\frac{1}{N}\sum_{j=1}^{N}[K_j(h)]^{p_i}\right\}^{1/p_i} \quad i = 1, 2, or\ 3 \qquad \textbf{(Eq. 3)}$$

where:

j = the sample index

N = the number of samples

$K_j(h)$ = the hydraulic conductivity of the j^{th} sample as a function of h

and the power p varies between −1 and 1.

The use of a larger p yields a larger $K^e(h)$ for a given data set. The averaging is equivalent to the arithmetic mean for $p = 1$ and the harmonic mean for $p = -1$; it approaches the geometric mean when p approaches zero. For $p_i = 1/3$, $K_1^e(h) = K_2^e(h) = K_3^e(h)$ and the power model is equivalent to the effective hydraulic conductivity of an isotropic EHM under 3D flow (Matheron, 1967, "Eléments pour une Théorie des Milieux Poreux" and Ababou, 1996, "Random Porous Media Flow on Large 3-D Grids: Numerics, Performance, and Application to Homogenization"). However, for the combined PA-TCT approach, p_i is not necessarily equal to 1/3 for the isotropic media. For brevity, the subscript i in $K_i^e(h)$ is omitted if it represents the effective conductivity in a principal direction.

Using Equation 3, the effective hydraulic conductivities of an EHM corresponding to different pressure heads are obtained as discrete K_i^e versus h data pairs. Data pairs in the i^{th} principal direction are described by the TCT model (Zhang et al., 2003):

$$K_i^e(h) = K_{si}^e[S^e(h)]^{L_i^e} B^e(h,\beta,\gamma) \quad i = 1,2, or\ 3 \qquad \textbf{(Eq. 4)}$$

where:

K_s^e = the effective hydraulic conductivity of an EHM at full saturation

L^e = the effective connectivity-tortuosity coefficient and $S^e(h) = [\theta(h)^e - \theta_r^e)]/(\theta_s^e - \theta_r^e)$ is the effective saturation

$\theta(h)^e$ = the effective volumetric water content as a function of matric potential h

θ_s^e = the effective volumetric water content at full saturation

θ_r^e = the effective residual volumetric water content, and $B^e(h,\beta,\gamma)$ is the contribution of effective water retention to $K_i^e(h)$ and is defined by Equation 5 as follows:

$$B^e(h,\beta,\gamma) = \left[\int_0^{S^e}\left(h^{-\beta} dS^e\right) \Big/ \int_0^1 \left(h^{-\beta} dS^e\right) \right]^\gamma \qquad \textbf{(Eq. 5)}$$

where β and γ are empirical constants. $B^e(h,\beta,\gamma)$ equals 1 when $S^e = 1$ and zero when $S^e = 0$ regardless of the values for β and γ and becomes smaller with decreasing saturation. Equation 5 corresponds to Burdine's model (Burdine, 1953, "Relative Permeability Calculation from Pore-Size Distribution Data"), when $\beta = 2$ and $\gamma = 1$ and to Mualem's (1976) model when $\beta = 1$ and $\gamma = 2$.

Equation 4 implies that the directional unsaturated hydraulic conductivity is a symmetric second-order tensor, $\mathbf{K}^e(h)$, and is the product of a scalar variable, the symmetric connectivity-tortuosity tensor $\mathbf{T}(h, L_i^e)$, and the hydraulic conductivity tensor at saturation, $\mathbf{K_s}^e$ (Raats et al., 2004, "The Relative connectivity-Tortuosity Tensor for conduction of Water in Anisotropic Unsaturated Soils"):

$$\boldsymbol{K}^e(h) = B^e(h,\beta,\gamma)\ \boldsymbol{T}(h, L_i^e)\ \boldsymbol{K}_s^e \qquad \textbf{(Eq. 6)}$$

Equation 6 shows that the TCT model also applies to the field-scale effective hydraulic conductivity for anisotropic media. Note that, at full saturation, the relative connectivity-tortuosity tensor $\mathbf{T}(h, L_i^e)$ reduces to the unit second-order tensor $\mathbf{I}$, i.e., $\mathbf{T}(S_e = 1, L_i^e) = \mathbf{I}$.

To summarize, using an appropriate p_i in the i^{th} principal direction and Equation 3, the directional effective hydraulic conductivity, $K_i^e(h)$, is first obtained as a function of pressure head at discrete h values. Together with the effective retention curve, the Equation 3-based $K_i^e(h)$ data pairs are described next with the TCT model, Equation 4, by fitting the effective connectivity-tortuosity coefficient L_i^e. A more detailed procedure for the PA-TCT model calculations is presented in Chapter 8.

5.4 Testing and Evaluation of the Variable Anisotropy Model

Using the combined PA-TCT model, Zhang and Khaleel (2010) estimated the 3D effective unsaturated hydraulic conductivity tensor for the Sisson and Lu (S&L) field injection site in the 200 East Area. Details of the S&L site, field injections, and the spatio-temporal distribution of observed moisture plume are described elsewhere (Ye et al., 2005, "Stochastic Analysis of Moisture Plume Dynamics of a Field Injection Experiment"; Zhang and Khaleel, 2010). Zhang and Khaleel (2010) present the results of testing and evaluation of the variable anisotropy model using the 200 East Area S&L field injection site moisture plume data. Overall, the PA-TCT model-based numerical simulation results using mild anisotropy compared well with the observed plume behavior at the S&L site (Zhang and Khaleel 2010).

6 Physical and Hydraulic Properties for the Laboratory-Measured Core Samples

As stated earlier, for the heterogeneous unsaturated media, the small-scale laboratory measurements on hydraulic properties are used to simulate the large, field-scale behavior. Each heterogeneous geologic unit is replaced by an EHM with upscaled or effective (macroscopic) flow properties.

6.1 Particle Size Distribution Data

The hydraulic property of a bulk sediment sample is fundamentally impacted by the sediment PSD. The determination of relative amounts of gravel, sand, and mud (silt and clay) content is therefore an important step in determination of hydraulic characteristics for a given HSU.

Figure 5 and Figure 6 illustrate the differences in sediment PSD for samples in the 200 East and 200 West Areas for a few representative sites (Figure 7 and Figure 8). These plots are based on the ROCkwell Hanford Operations Sediment Analysis (ROCSAN) database (Hanford Virtual Library) for borehole sediment samples, the majority being representative of the Hanford formation. The relative fraction of gravel, sand, and mud content along with their ranges is estimated based on grain-size distribution data derived from sieve analysis. Overall, as the histogram plots show, the 200 West Area sediment samples are considerably finer than the 200 East Area samples; this is illustrated by the number and percentage of fine fraction in the histogram plots. This fundamental difference in sediment characteristics prompted separation of the 200 East and 200 West Area laboratory core samples for assigning hydraulic properties.

6.2 Sediment Sampling Sites

Figure 9 (1 of 2) shows the location of borehole sediment sampling sites in 200 East and 200 West Areas. The sediment samples from these sites were used to develop the hydraulic properties for different HSUs. Figure 9 (2 of 2) shows the borehole sediment sampling sites in the 300 and 100 Areas. Because of lack of samples for the gravel-dominated unit in the 200 East Area, the gravelly samples for the 100 and 300 Areas are used as surrogates.

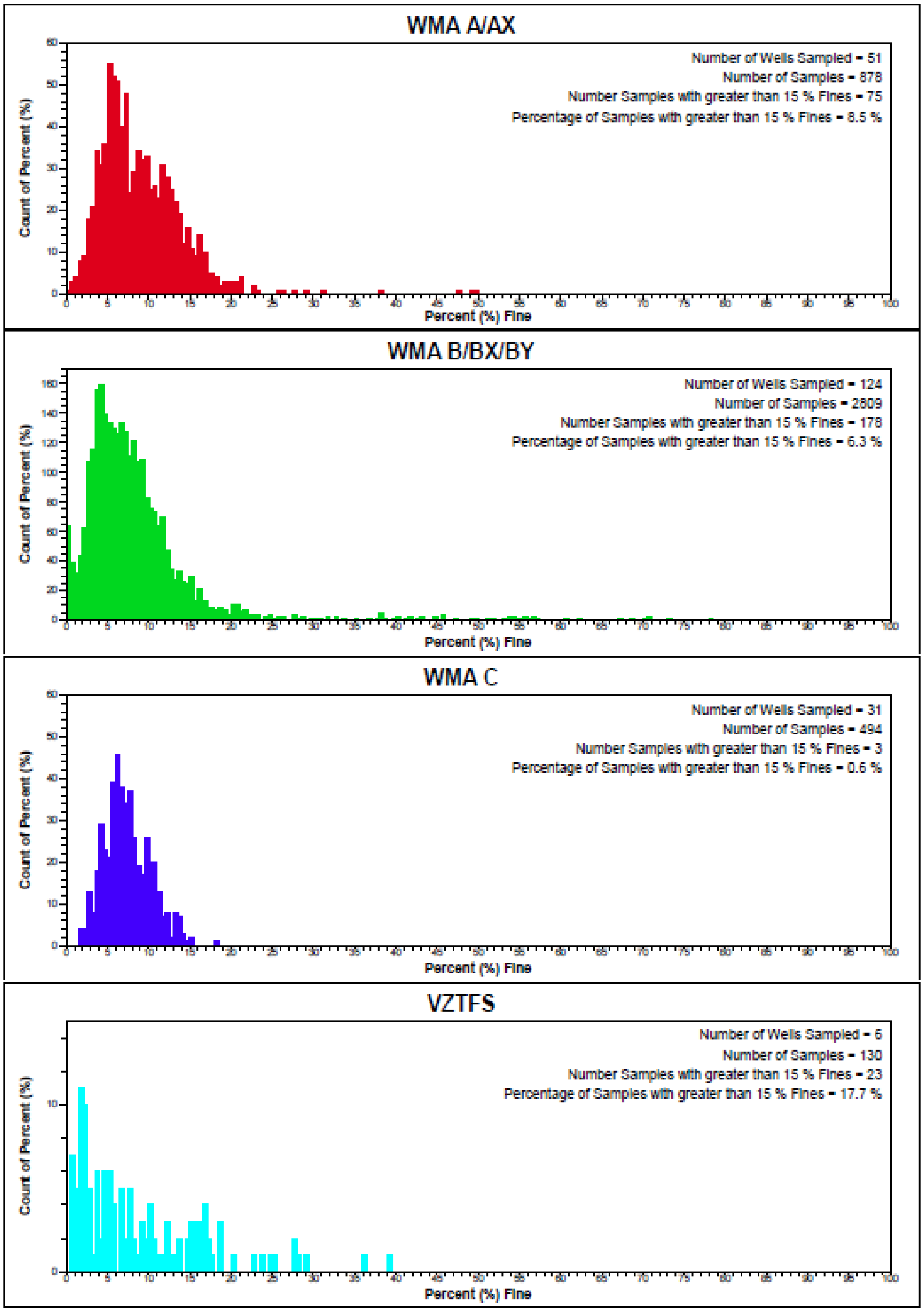

Figure 5. Histograms Illustrating Contrast in ROCSAN Database Derived Percent Fines for Selected Sites in the 200 East Area

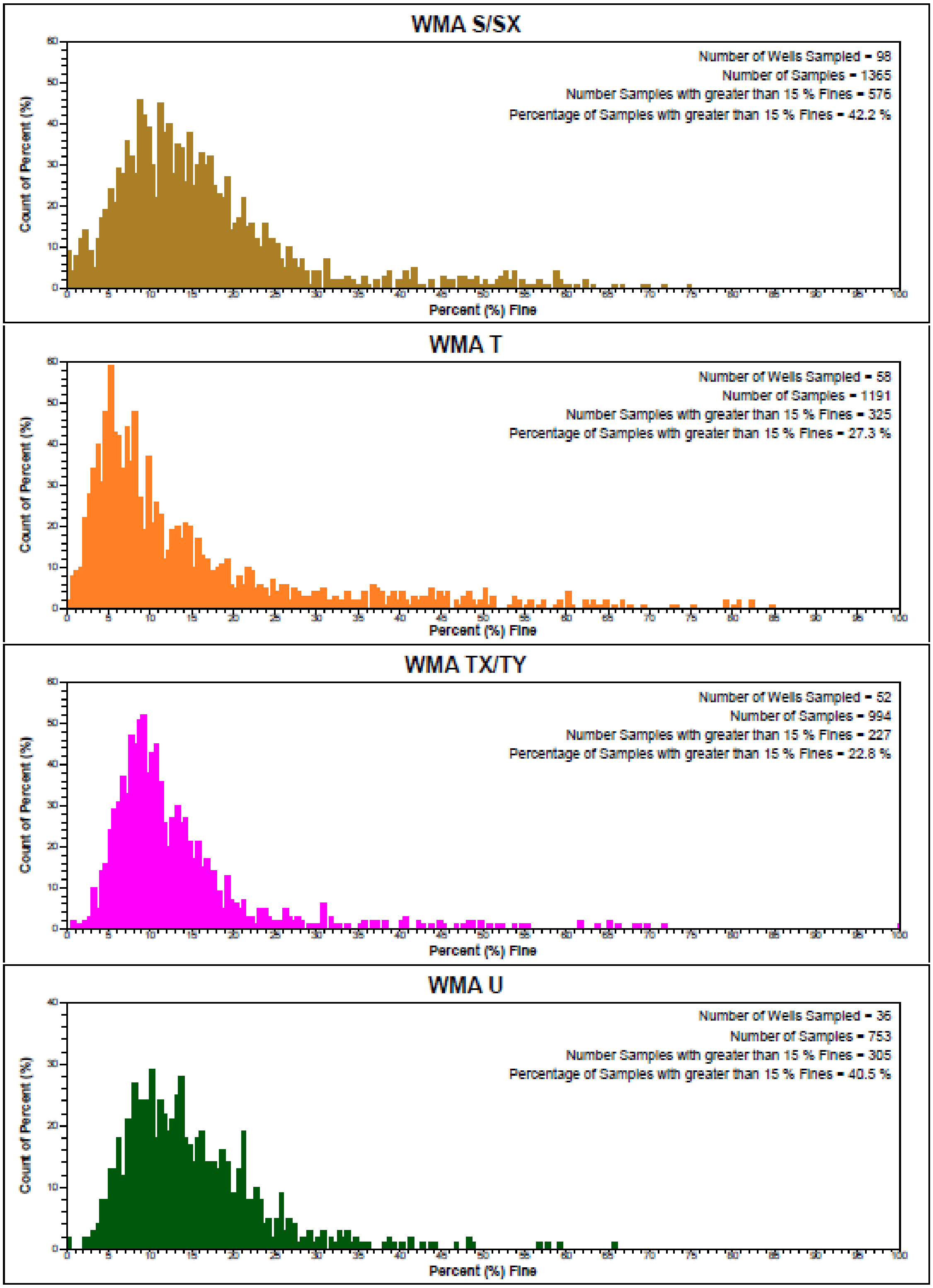

Figure 6. Histograms Illustrating Contrast in ROCSAN Database Derived Percent Fines for Selected Sites in the 200 West Area

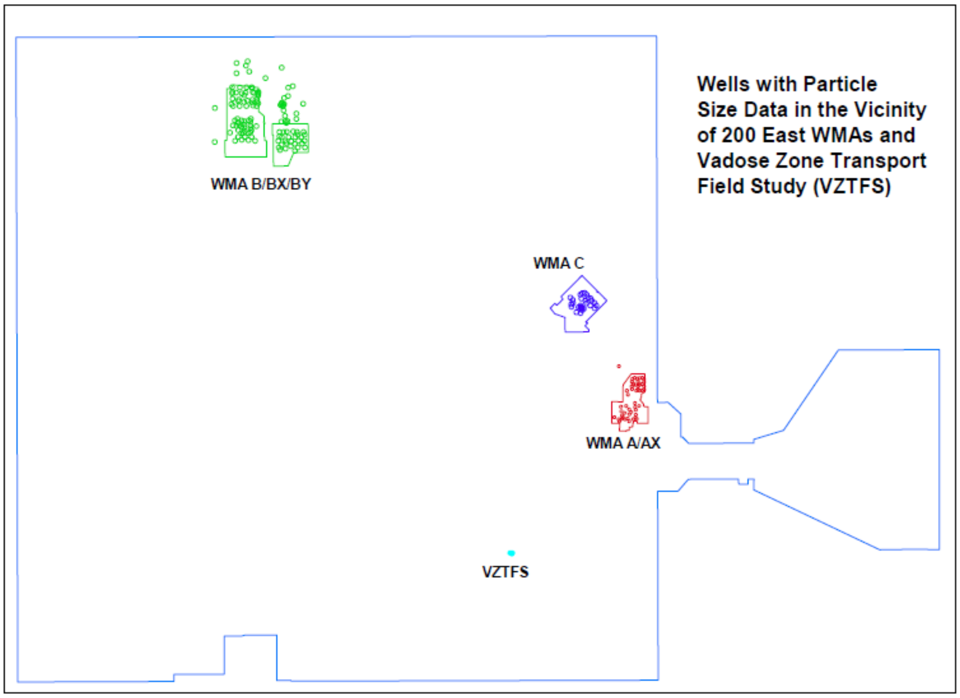

Figure 7. Location of Selected Sites in the 200 East Area

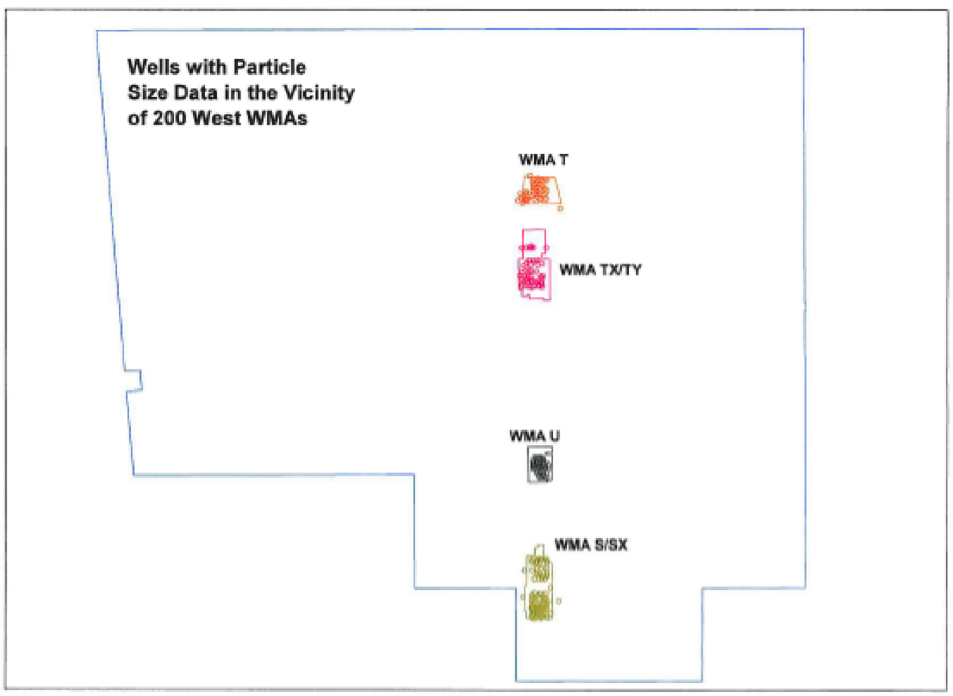

Figure 8. Location of Selected Sites in the 200 West Area

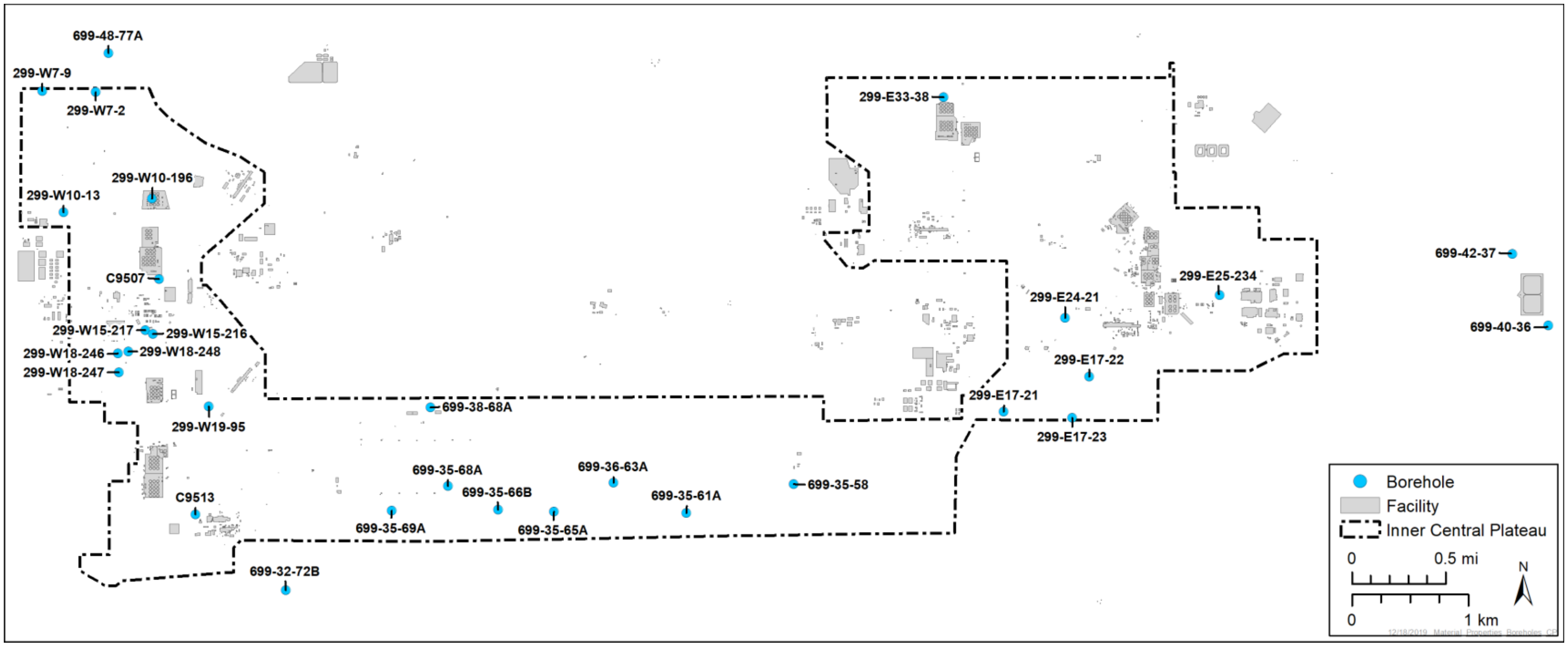

Figure 9. Location of Borehole Sediment Sampling Sites Used in Developing the Hydraulic Properties for Various Hydrostratigraphic Units (1 of 2)

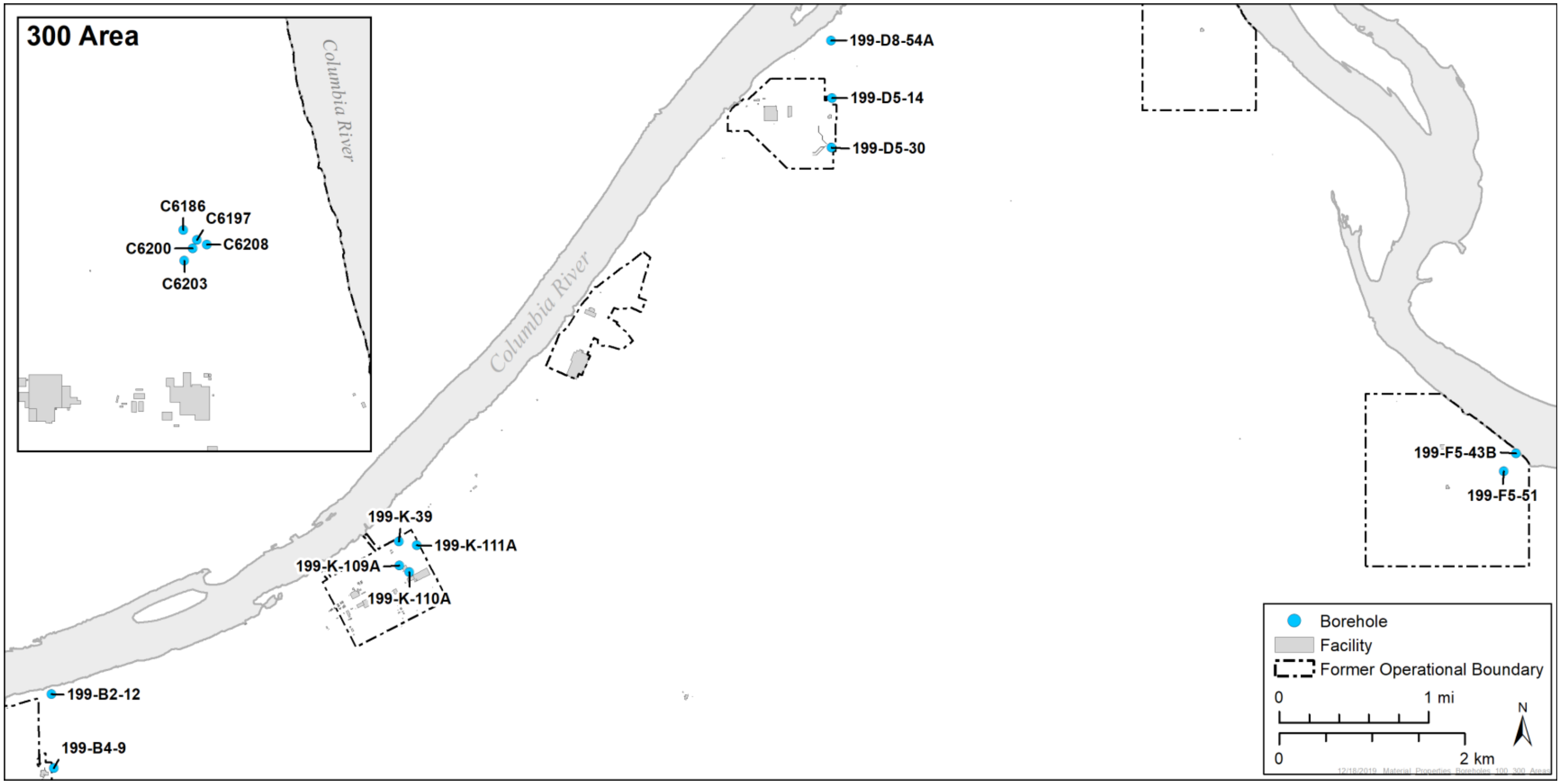

Figure 9. Location of Borehole Sediment Sampling Sites Used in Developing the Hydraulic Properties for Various Hydrostratigraphic Units (2 of 2)

6.3 Laboratory-Measured Properties for the 200 East Area Sediments

Based on a comparison of PSD for the individual sediment samples and the ROCSAN database, the properties for the HSUs in the 200 East Area are presented below as three combined grouping of units (i.e., sand-dominated, gravel-dominated, and fine-textured units):

- Sand-dominated units
  - Eolian sand
  - Hanford formation unit 2 (Hf2)
  - Cold Creek unit (CCU) sand
- Gravel-dominated units
  - Backfill
  - Hanford formation unit 1 (Hf1)
  - Hanford formation unit 3 (Hf3)
  - Cold Creek unit gravel (CCUg)
  - Ringold Formation member of Wooded Island – unit E (Rwie)
  - Ringold Formation member of Wooded Island – unit A (Rwia)
- Fine-textured Units
  - Cold Creek unit silt (CCUz)
  - Ringold lower mud

Table 1 through Table 4 list the derived van Genuchten model parameters and saturated hydraulic conductivity estimates for the samples used to represent the 200 East Area HSUs. Table 2 is based on RPP-20621, *Far-Field Hydrology Data Package for the Integrated Disposal Facility Performance Assessment*; the samples were collected as part of site characterization and drilling activities for the Integrated Disposal Facility (IDF). The drilling campaigns encountered open-framework gravel and were not able to collect samples below the sand-dominated unit. The gravelly samples for the 100 and 300 Areas are therefore used as surrogates for the gravel-dominated unit in the 200 East Area (Table 3).

Because of lack of data, the 200 West Area CCUz and Ringold lower mud unit samples are used to represent those two units in the 200 East Area as well (Table 4). No laboratory measurements are available for the B Complex CCU sand unit; it is assumed to be comprised of fine-textured sand and the S&L site samples for unit E (Zhang and Khaleel, 2010) are used as surrogates for the CCU sand unit.

6.4 Laboratory-Measured Properties for the 200 West Area Sediments

Similar to the 200 East Area, the properties for the HSUs in the 200 West Area are presented below as three combined grouping of units (i.e., sand-dominated, gravel-dominated, and fine-textured units):

- Sand-dominated units
  - Hf2
  - Ringold Formation member of Taylor Flat (Rtf)
- Gravel-dominated units
  - Backfill
  - Hf1
  - Hf3
  - Rwie
  - Rwia

- Fine-textured units
  - CCUz
  - Cold Creek unit caliche (CCUc)
  - Ringold lower mud

Table 5 through Table 9 list the derived van Genuchten model parameters and saturated hydraulic conductivity estimates for the samples used to represent the HSUs in the 200 West Area. Figure 9 illustrates the location maps for the samples listed in Table 1 through Table 9.

7 200 East Area B Complex Perched Water Aquifer Properties

Hydrogeologic conditions for the perched water aquifer (PWA) within the B Complex area are described elsewhere (e.g., PNNL-19277, *Conceptual Models for Migration of Key Groundwater Contaminants Through the Vadose Zone and into the Unconfined Aquifer Below the B-Complex*). Briefly, the primary hydrogeologic units comprising the PWA system include the CCUz-sand (the aquifer unit comprised of silty sand), and the overlying and underlying low-permeability CCUz-lower and CCUz-upper units (primarily comprised of silt). Underlying the CCUz-lower perching layer is the CCUg, which generally exhibits higher permeability than the CCUz-sand and is part of the regional Hanford Site unconfined aquifer system.

The PWA hydraulic properties reported in Table 10 are based on PNNL-27846, *Physical and Hydraulic Properties of Sediments from the 200-DV-1 Operable Unit*. These properties are representative of the PWA CCUz-sand, and were obtained from hydrologic (i.e., slug) tests conducted at PWA wells 299-E33-344, 299-E33-350, and 299-E33-351 during fiscal years 2014, 2016, and 2017 (PNNL-27846).

8 Effective (Upscaled) Flow Parameters for Hydrostratigraphic Units

Each HSU was treated as an anisotropic EHM whose effective hydraulic properties were estimated using the available core-scale data (Chapter 6). This chapter discusses how the effective retention parameters and the directional unsaturated conductivity (K) parameters were obtained for each HSU. Effective transport parameters are discussed in Chapter 9.

8.1 Effective Soil Moisture Retention

A simple averaging of soil moisture data (Table 1 through Table 4 and Table 5 through Table 9) were used to define the effective saturated and residual moisture contents for the HSUs in the 200 East and 200 West Areas. A linear averaging scheme (Green et al., 1996, "Upscaled Soil-Water Retention Using van Genuchten's Function") in Equation 7 was used to describe the effective soil-water saturation $S^e(h)$ at a given pressure head h:

$$S^e(h) = \frac{1}{N} \sum_{j=1}^{N} S_j(h) \qquad \textbf{(Eq. 7)}$$

The effective retention curves were next described by van Genuchten's (1980) soil moisture retention model shown in Equation 8:

$$S^e(h) = \left[1 + (\alpha^e|h|)^{n^e}\right]^{\left(1/n^e - 1\right)} \qquad \textbf{(Eq. 8)}$$

where α^e and n^e are the effective van Genuchten parameters. Further details on the calculation procedure are described in Section 8.2.

Table 1. van Genuchten Parameter Values and Saturated Hydraulic Conductivities for the 12 Borehole Samples Used to Represent the 200 East Area Eolian Sand

Data Source	Sample	Site/ Operable Unit	Borehole Number	Depth (m bgs)	Gravel Content (% wt)	θ_s (cm^3/cm^3)	θ_r (cm^3/cm^3)	α (1/cm)	n (-)	K_s (cm/s)
WCH-EP-0883	5A	Grout Well Site	299-E25-234	1.5	1	0.4131	0.0187	0.148	1.3087	5.73E-04
WCH-EP-0883	5B	Grout Well Site	299-E25-234	1.5	1	0.3367	0.0336	0.0211	1.536	5.73E-04
WCH-EP-0883	19A	Grout Well Site	299-E25-234	5.8	2	0.486	0.0461	0.387	1.2615	8.88E-04
WCH-EP-0883	19B	Grout Well Site	299-E25-234	5.8	2	0.5026	0.0363	0.2729	1.5326	8.88E-04
WCH-EP-0883	25A	Grout Well Site	299-E25-234	7.6	0	0.4407	0.0539	0.0473	2.0595	1.80E-03
WCH-EP-0883	25B	Grout Well Site	299-E25-234	7.6	0	0.5228	0.0342	0.0519	1.3421	1.80E-03
WCH-EP-0883	25C	Grout Well Site	299-E25-234	7.6	0	0.5062	0.028	0.0287	1.3529	1.80E-03
WCH-EP-0883	25D	Grout Well Site	299-E25-234	7.6	0	0.4822	0.08	0.07	1.878	1.80E-03
WCH-EP-0883	29A	Grout Well Site	299-E25-234	8.8	0	0.4341	0	0.2718	1.1928	2.41E-05
WCH-EP-0883	29B	Grout Well Site	299-E25-234	8.8	0	0.4387	0	0.1033	1.2242	2.41E-05
WCH-EP-0883	37A	Grout Well Site	299-E25-234	11.3	1	0.5114	0.0703	0.0775	1.2921	5.77E-04
WCH-EP-0883	37B	Grout Well Site	299-E25-234	11.3	1	0.5304	0.0844	0.0914	1.3319	5.77E-04

Reference: WHC-EP-0883, *Variability and Scaling of Hydraulic Properties for 200 Area Soils, Hanford Site*.

bgs = below ground surface

Table 2. van Genuchten Parameter Values and Saturated Hydraulic Conductivities for the 44 Borehole Samples Used to Represent the 200 East Area Hanford formation Unit 2

Data Source	Sample	Site/ Operable Unit	Borehole Number	Depth (m bgs)	Gravel Content (% wt)	θs (cm^3/cm^3)	θr (cm^3/cm^3)	α (1/cm)	*n* (-)	K_s (cm/s)
RPP-20621	7A	IDF	299-E17-21	14.0-14.6	0.2	0.377	0.0404	0.029	1.825	1.04E-03
RPP-20621	10A	IDF	299-E17-21	17.6-18.2	0	0.413	0.0279	0.1161	1.784	2.95E-03
RPP-20621	12A	IDF	299-E17-21	21.2-21.6	0.7	0.363	0.0309	0.065	1.755	2.15E-03
RPP-20621	14A	IDF	299-E17-21	24.5-25.2	0.2	0.416	0.0324	0.0445	1.728	1.99E-03
RPP-20621	15A	IDF	299-E17-21	27.6-28.3	0.5	0.38	0.0254	0.0487	1.844	2.09E-03
RPP-20621	16A	IDF	299-E17-21	30.6-31.4	1.5	0.42	0.0228	0.0682	1.71	9.57E-03
RPP-20621	17A	IDF	299-E17-21	33.5-34.2	0.3	0.423	0.0382	0.0689	1.899	1.99E-03
RPP-20621	19A	IDF	299-E17-21	36.9-37.6	0	0.444	0.0279	0.201	1.542	4.31E-03
RPP-20621	20A	IDF	299-E17-21	39.5-40.2	0.2	0.419	0.0321	0.0305	2.081	2.54E-03
RPP-20621	21A	IDF	299-E17-21	43.1-43.9	0.4	0.403	0.0276	0.0545	1.926	2.94E-03
RPP-20621	22A	IDF	299-E17-21	46.3-47.1	1.6	0.352	0.0252	0.1078	1.585	5.06E-03
RPP-20621	23A	IDF	299-E17-21	48.9-49.7	0	0.371	0.0411	0.0079	1.553	2.65E-04
RPP-20621	24A	IDF	299-E17-21	55.1-55.7	0.2	0.321	0.0413	0.013	1.684	5.69E-04
RPP-20621	25A	IDF	299-E17-21	57.8-58.4	0.3	0.345	0.0267	0.0842	2.158	5.40E-03
RPP-20621	27A	IDF	299-E17-21	60.7-61.4	1.7	0.377	0.0354	0.083	1.532	8.14E-03
RPP-20621	29A	IDF	299-E17-21	63.8-64.4	1.2	0.359	0.0317	0.0784	1.732	3.75E-03
RPP-20621	31A	IDF	299-E17-21	66.9-67.5	0.2	0.418	0.0444	0.0058	2.012	8.21E-04
RPP-20621	32A	IDF	299-E17-21	68.9-69.5	1.8	0.359	0.0401	0.0931	1.703	6.71E-03
RPP-20621	34A	IDF	299-E17-21	72.0-72.6	13	0.316	0.0324	0.0819	2.398	1.32E-02
RPP-20621	35A	IDF	299-E17-21	73.0-73.6	24.3	0.299	0.0428	0.0897	2.16	1.06E-02
RPP-20621	45L	IDF	299-E24-21	13.7-14.3	4.1	0.385	0.008	0.1039	1.737	3.24E-02
RPP-20621	45U	IDF	299-E24-21	13.7-14.3	4.1	0.385	0.005	0.088	1.664	3.24E-02
RPP-20621	50L	IDF	299-E24-21	15.2-15.8	1.9	0.42	0.025	0.073	1.71	1.75E-03
RPP-20621	50U	IDF	299-E24-21	15.2-15.8	1.9	0.42	0.013	0.045	1.667	1.75E-03

Table 2. van Genuchten Parameter Values and Saturated Hydraulic Conductivities for the 44 Borehole Samples Used to Represent the 200 East Area Hanford formation Unit 2

Data Source	Sample	Site/ Operable Unit	Borehole Number	Depth (m bgs)	Gravel Content (% wt)	θs (cm^3/cm^3)	θr (cm^3/cm^3)	α (1/cm)	*n* (-)	K_s (cm/s)
RPP-20621	80L	IDF	299-E24-21	24.4-25.0	13	0.359	0.031	0.0403	2.368	1.05E-03
RPP-20621	80U	IDF	299-E24-21	24.4-25.0	13	0.359	0.033	0.0313	2.572	1.05E-03
RPP-20621	85L	IDF	299-E24-21	25.9-26.5	3.6	0.406	0.023	0.1074	1.697	3.84E-02
RPP-20621	85U	IDF	299-E24-21	25.9-26.5	3.6	0.406	0.027	0.0847	1.595	3.84E-02
RPP-20621	110L	IDF	299-E24-21	33.5-34.1	0.4	0.412	0.039	0.0362	2.328	5.16E-04
RPP-20621	110U	IDF	299-E24-21	33.5-34.1	0.4	0.412	0.046	0.0268	3.182	5.16E-04
RPP-20621	130L	IDF	299-E24-21	39.6-40.2	9.8	0.358	0.032	0.094	2.003	1.97E-02
RPP-20621	130U	IDF	299-E24-21	39.6-40.2	9.8	0.358	0.036	0.0674	1.934	1.97E-02
RPP-20621	150L	IDF	299-E24-21	45.7-46.3	1.7	0.431	0.015	0.0992	1.547	7.48E-03
RPP-20621	150U	IDF	299-E24-21	45.7-46.3	1.7	0.431	0.024	0.0703	1.514	7.48E-03
RPP-20621	200L	IDF	299-E24-21	61.0-61.6	2.9	0.41	0.002	0.0995	2.162	4.93E-02
RPP-20621	215L	IDF	299-E24-21	65.5-66.1	13.4	0.37	0.028	0.0448	1.918	2.24E-03
RPP-20621	215U	IDF	299-E24-21	65.5-66.1	13.4	0.37	0.023	0.0333	1.815	2.24E-03
RPP-20621	230L	IDF	299-E24-21	70.1-70.7	31.9	0.309	0.04	0.0472	1.658	3.56E-03
RPP-20621	230U	IDF	299-E24-21	70.1-70.7	31.9	0.309	0.038	0.04	1.658	3.56E-03
RPP-20621	251L	IDF	299-E24-21	76.5-76.8	3	0.427	0.032	0.084	1.845	1.43E-02
RPP-20621	261L	IDF	299-E24-21	79.7-80.3	0.7	0.39	0.045	0.0191	2.485	5.54E-04
RPP-20621	C3826-171	IDF	299-E17-22	52.1-52.4	0	0.382	0.0226	0.039	1.84	7.96E-03
RPP-20621	C3827-63.5	IDF	299-E17-23	19.4-19.7	0	0.444	0	0.0914	1.5	2.23E-02
RPP-20621	C3827-221	IDF	299-E17-23	67.4-67.7	0	0.361	0.022	0.066	1.77	7.30E-03

Reference: RPP-20621, *Far-Field Hydrology Data Package for the Integrated Disposal Facility Performance Assessment*.

bgs = below ground surface

IDF = Integrated Disposal Facility

L = lower portion of sample

U = upper portion of sample

Table 3. van Genuchten Parameters Values and Saturated Hydraulic Conductivities for the 25 Borehole Samples Used to Represent the 200 East Area Gravelly Units

Data Source	Sample	Site/ Operable Unit	Borehole Number	Depth (m bgs)	Gravel Content (% wt)	θ_s (cm^3/cm^3)	θ_r (cm^3/cm^3)	α (1/cm)	n (-)	K_s (cm/s)
RPP-20621	2-1307	100-HR-3	199-D5-14	18.90	43	0.236	0.0089	0.013	1.447	1.290E-04
RPP-20621	2-1308	100-HR-3	199-D5-14	30.64	58	0.12	0.0208	0.0126	1.628	6.970E-05
RPP-20621	2-1318	100-HR-3	199-D8-54A	15.54	60	0.124	0.0108	0.0081	1.496	1.670E-04
RPP-20621	2-2663	100-BC-5	199-B2-12	8.2	61	0.135	0.0179	0.0067	1.527	6.730E-05
RPP-20621	2-2664	100-BC-5	199-B2-12	24.84	73	0.125	0.0136	0.0152	1.516	1.120E-04
RPP-20621	2-2666	100-BC-5	199-B4-9	21.49	71	0.138	0	0.0087	1.284	1.020E-04
RPP-20621	2-2667	100-BC-5	199-B4-9	23.93	75	0.094	0	0.0104	1.296	1.400E-04
RPP-20621	3-0570	100-KR-1	116-K-39	3.50	60	0.141	0	0.0869	1.195	2.060E-02
RPP-20621	3-0577	100-KR-3	199-F5-43B	7.16	66	0.107	0	0.0166	1.359	2.490E-04
RPP-20621	3-0686	100-FR-3	116-F5-51	6.49	55	0.184	0	0.0123	1.6	5.930E-04
RPP-20621	3-1702	100-FR-1	199-D5-30	9.78	68	0.103	0	0.0491	1.26	1.300E-03
RPP-20621	4-1086	100-K	199-K-110A	12.77	65	0.137	0	0.1513	1.189	5.830E-02
RPP-20621	4-1090	100-K	199-K-111A	8.20	50	0.152	0.0159	0.0159	1.619	4.050E-04
RPP-20621	4-1118	100-K	199-K-109A	10.30	66	0.163	0	0.2481	1.183	3.890E-02
RPP-20621	4-1120	100-K	199-K-109A	18.90	63	0.131	0.007	0.0138	1.501	2.850E-04
PNNL-22886	C6186,18.4-19.4	IFRC	C6186	5.6-5.9	82	0.152	0	0.0388	1.378	2.83E-04
PNNL-22886	C6197,27-28	IFRC	C6197	8.2-8.5	68	0.176	0	0.115	1.324	4.33E-04
PNNL-22886	C6197,42-43	IFRC	C6197	12.8-13.1	67	0.178	0	0.0929	1.366	2.61E-02
PNNL-22886	C6197,51-52	IFRC	C6197	15.5-15.8	56	0.214	0	0.0435	1.272	5.43E-05
PNNL-22886	C6200,21-22	IFRC	C6200	6.4-6.7	89	0.219	0	0.0626	1.383	2.85E-01
PNNL-22886	C6203,16-17	IFRC	C6203	4.9-5.2	81	0.213	0	0.358	1.195	1.06E-01
PNNL-22886	C6203,20-21	IFRC	C6203	6.1-6.4	79	0.285	0	0.2286	1.269	3.72E-03
PNNL-22886	C6203,35.8-36.8	IFRC	C6203	10.9-11.2	72	0.302	0	2.4189	1.299	3.26E-02

Table 3. van Genuchten Parameters Values and Saturated Hydraulic Conductivities for the 25 Borehole Samples Used to Represent the 200 East Area Gravelly Units

Data Source	Sample	Site/ Operable Unit	Borehole Number	Depth (m bgs)	Gravel Content (% wt)	θ_s (cm³/cm³)	θ_r (cm³/cm³)	α (1/cm)	n (-)	K_s (cm/s)
PNNL-22886	C6203,40-41	IFRC	C6203	12.2-12.5	45	0.266	0	0.2733	1.509	1.30E-02
PNNL-22886	C6208,23-24	IFRC	C6208	7.0-7.3	77	0.246	0	0.1479	1.201	2.13E-02

References: RPP-20621, *Far-Field Hydrology Data Package for the Integrated Disposal Facility Performance Assessment*.

PNNL-22886, *System-Scale Model of Aquifer, Vadose Zone, and River Interactions for the Hanford 300 Area – Application to Uranium Reactive Transport*.

Note: Gravelly units include Backfill, Hanford formation units 1 and 3, Cold Creek unit gravel, Ringold Formation member of Wooded Island – unit E, and Ringold Formation member of Wooded Island – unit A.

bgs = below ground surface

IFRC = Integrated Field Research Challenge

Table 4. van Genuchten Parameter Values and Saturated Hydraulic Conductivities for the 11 Borehole Samples Used to Represent the 200 East Area Cold Creek Unit Silt and 200 West Area Cold Creek Unit Silt and Ringold Lower Mud Units

Data Source	Sample	Site/Operable Unit	Borehole Number	Depth (m bgs)	Gravel Content (% wt)	θ_s (cm^3/cm^3)	θ_r (cm^3/cm^3)	α (1/cm)	n (-)	K_s (cm/s)
WHC-EP-0883	1-0530	200-BP-1	299-E33-38	57.1	0	0.2663	0.0098	0.0123	1.6899	7.10E-05
Khaleel et al. (1995)	0-080	218-W-5	299-W7-9	21.57	0	0.367	0.04	0.0061	3.435	7.90E-04
Khaleel et al. (1995)	0-079	218-W-5	299-W7-9	21.11	0	0.375	0	0.0063	1.995	6.70E-05
Khaleel et al. (1995)	0-072	218-W-5	299-W7-9	19.82	0	0.328	0.052	0.0067	2.317	6.00E-04
WHC-EP-0883	3-0647	VOC	299-W18-246	42.9	0	0.4995	0.04	0.0051	2.053	2.00E-04
WHC-EP-0883	3-0649	VOC	299-W18-247	41.1	0	0.5331	0.06	0.001	1.7024	9.96E-05*
PNNL-27846	B35435	T Complex/216-T-19 Crib & Tile Field	C9507	31.2	0	0.4075	0.1265	0.0049	2.1334	1.03E-04
WHC-EP-0645	0-080	218-W-5	299-W7-9	21.57	0	0.4257	0.047	0.0061	3.4887	2.51E-05
WHC-EP-0645	0-073	218-W-5	299-W7-9	20.27	0	0.4124	0.089	0.0008	2.1917	4.01E-07
WHC-EP-0645	0-072	218-W-5	299-W7-9	19.82	0	0.3905	0.056	0.009	2.0877	5.43E-05
WHC-EP-0645	0-079	218-W-5	299-W7-9	21.11	0	0.3881	0.076	0.0077	2.4196	1.43E-05

Note: Complete references are provided in Chapter 11.

*Not available. K_s estimate based on averaging of preceding five samples.

bgs = below ground surface

VOC = volatile organic compound

Table 5. van Genuchten Parameter Values and Saturated Hydraulic Conductivities for the 18 Borehole Samples Used to Represent the 200 West Area Hanford formation Unit 2

Data Source	Sample	Site/ Operable Unit	Borehole Number	Depth (m bgs)	Gravel Content (% wt)	θ_s (cm^3/cm^3)	θ_r (cm^3/cm^3)	α (1/cm)	n (-)	K_s (cm/s)
WCH-464	3-0589	241-T-106	299-W10-196	25.5	1	0.429	0.0268	0.0057	1.7173	4.73E-05
WCH-464	3-1707	200-UP-2	299-W19-95	9.5	15	0.364	0.0742	0.0082	2.0349	1.55E-05
WCH-464	3-1712	200-UP-2	299-W19-95	43.1	0	0.290	0.0362	0.0156	2.021	2.05E-04
WCH-464	3-1713	200-UP-2	299-W19-95	46.3	0	0.5026	0	0.0077	1.6087	2.51E-05
WCH-464	3-1714	200-UP-2	299-W19-95	50.8	2	0.394	0.1301	0.0061	1.535	1.05E-04
WCH-464	4-0637	ERDF	699-36-63A	74.9	0	0.378	0	0.0153	1.7309	6.89E-05
WCH-464	4-0642	ERDF	699-35-69A	25.7	0	0.353	0.0286	0.014	1.4821	6.81E-04
WCH-464	4-0644	ERDF	699-35-69A	49.8	0	0.394	0.0557	0.0076	1.8353	3.24E-05
WCH-464	4-0791	ERDF	699-35-65A	63.2	0	0.338	0.0256	0.0226	2.2565	6.81E-04
WCH-464	4-1076	ERDF	699-35-61A	76.4	0	0.357	0	0.0293	1.7015	1.23E-03
WCH-464	4-1111	200-UP-1	699-38-68A	56.9	1	0.394	0.0497	0.0093	1.4342	5.80E-05
WCH-464	4-1112	200-UP-1	699-38-68A	66.0	0	0.4346	0	0.0054	1.4985	2.49E-05
WHC-EP-0883	3-0652	VOC	299-W18-248	38.4	0	0.3586	0.03	0.0092	1.8848	3.70E-04
WHC-EP-0883	4-0973	ERDF	699-35-68A	37.0	0	0.3525	0.019	0.0169	2.0085	1.27E-04
WHC-EP-0883	4-1056	ERDF	699-32-72B	61.7	0	0.4288	0.035	0.0071	2.7253	N/A
WHC-EP-0883	4-1057	ERDF	699-32-72B	49.5	0	0.4877	0.089	0.0046	2.2861	N/A
WHC-EP-0883	4-1058	ERDF	699-32-72B	64.7	0	0.5661	0.1023	0.0029	1.5267	N/A
WHC-EP-0883	4-0855	ERDF	699-35-66B	12.2	0	0.3936	0.0689	0.0088	3.2652	N/A

References: WCH-464, *Hydrologic Data Package in Support of Environmental Restoration Disposal Facility Performance Assessment Modeling*.
WHC-EP-0883, *Variability and Scaling of Hydraulic Properties for 200 Area Soils, Hanford Site*.

bgs = below ground surface
ERDF = Environmental Restoration Disposal Facility
N/A = not available
VOC = volatile organic compound

Table 6. van Genuchten Parameter Values and Saturated Hydraulic Conductivities for the 11 Borehole Samples Used to Represent the 200 West Area Backfill and Hanford formation Units 1 and 3

Data Source	Sample	Site/ Operable Unit	Borehole Number	Depth (m bgs)	Gravel Content (% wt)	θ_s (cm^3/cm^3)	θ_r (cm^3/cm^3)	α (1/cm)	n (-)	K_s (cm/s)
WCH-464	3-0210	241-T-106	299-W10-196	3.1	48	0.186	0.029	0.014	1.7674	1.96E-04
WCH-464	3-0668	241-T-106	299-W10-196	38.9	62	0.175	0	0.0192	1.6124	1.63E-04
WCH-464	3-0682	241-T-106	299-W10-196	46.1	51	0.224	0	0.0166	1.6577	2.37E-04
WCH-464	3-0688	241-T-106	299-W10-196	48.5	49	0.199	0	0.0043	1.5321	2.60E-05
WCH-464	3-0689	241-T-106	299-W10-196	52.2	28	0.236	0	0.0025	1.4747	4.58E-05
WCH-464	3-0690	241-T-106	299-W10-196	53.7	53	0.1819	0.0177	0.0046	1.541	4.19E-05
WHC-EP-0645	0-069	218-W-5	299-W7-9	3.05	60	0.3005	0	0.0945	1.2515	2.06E-02
WHC-EP-0883	3-0001	W-049-H	699-40-36	29.3	68	0.1128	0.0156	0.0095	1.5556	1.82E-04
WHC-EP-0883	W10-13-80	218-W-5	299-W10-13	24.4	64	0.1781	0.0367	0.2758	1.3718	2.70E-02
WHC-EP-0883	2-3088	W-049-H	699-42-37	4.6	65	0.1071	0.0197	0.0038	1.5977	1.30E-03
WHC-EP-0883	3-0213	241-T-106	299-W10-196	5.6	31	0.2083	0.0494	0.004	2.4233	1.02E-03

References: WCH-464, *Hydrologic Data Package in Support of Environmental Restoration Disposal Facility Performance Assessment Modeling*.

WHC-EP-0645, *Performance Assessment for the Disposal of Low-Level Waste in the 200 West Area Burial Grounds*.

WHC-EP-0883, *Variability and Scaling of Hydraulic Properties for 200 Area Soils, Hanford Site*.

bgs = below ground surface

Table 7. van Genuchten Parameter Values and Saturated Hydraulic Conductivities for the 10 Borehole Samples Used to Represent the 200 West Area Rwie and Rwia Gravelly Units

Data Source	Sample	Site/ Operable Unit	Borehole Number	Depth (m bgs)	Gravel Content (% wt)	θs (cm^3/cm^3)	θr (cm^3/cm^3)	α (1/cm)	n (-)	Ks (cm/s)
WHC-EP-0883	W7-2-154	218-W-5	299-W7-2	46.9	32	0.3071	0.015	0.1027	1.3782	2.10E-02
WHC-EP-0883	W7-2-219	218-W-5	299-W7-2	66.8	39	0.1594	0.0617	0.0680	1.7788	2.70E-03
WHC-EP-0883	4-0983	ERDF	699-35-68A	82.9	17	0.3373	0.01	0.0156	2.0226	5.43E-05
WHC-EP-0883	4-1079	ERDF	699-35-61A	90.9	65	0.1236	0.0295	0.0073	1.6668	1.30E-03
WHC-EP-0883	3-0667	241-T-106	299-W10-196	42.2	80	0.0718	0	0.0115	1.3466	2.83E-05
WHC-EP-0883	3-0668	241-T-106	299-W10-196	38.9	63	0.147	0.01	0.0023	1.5765	1.60E-03
WHC-EP-0883	2-1432	C-018-H	699-48-77A	27.6	51	0.1128	0.0191	0.0083	1.5938	1.40E-02
WHC-EP-0883	3-0648	VOC	299-W18-246	59.6	62	0.1462	0	0.0124	1.645	8.70E-03
WHC-EP-0883	3-0656	VOC	299-W15-216	39.0	42	0.1814	0.009	0.0166	1.3941	1.36E-02
WHC-EP-0883	300	US Ecology	699-35-58	91.4	59	0.119	0.0123	0.0105	1.6304	7.66E-04

Reference: WHC-EP-0883, *Variability and Scaling of Hydraulic Properties for 200 Area Soils, Hanford Site.*

bgs = below ground surface

ERDF = Environmental Restoration Disposal Facility

Rwia = Ringold Formation member of Wooded Island – unit A

Rwie = Ringold Formation member of Wooded Island – unit E

VOC = volatile organic compound

Table 8. van Genuchten Parameter Values and Saturated Hydraulic Conductivities for the Eight Borehole Samples Used to Represent the 200 West Area Cold Creek Unit Caliche

Data Source	Sample	Site/ Operable Unit	Borehole Number	Depth (m bgs)	Gravel Content (% wt)	θ_s (cm^3/cm^3)	θ_r (cm^3/cm^3)	α (1/cm)	n (-)	K_s (cm/s)
Khaleel et al. (1995)	0-099	218-W-5	299-W7-9	30.26	0	0.338	0.039	0.0152	1.706	4.78E-04
WHC-EP-0883	0-085	218-W-5	299-W7-9	26.9	0	0.2105	0.0578	0.0049	2.1261	1.30E-04
Khaleel et al. (1995)	0-083	218-W-5	299-W7-9	24.92	0	0.349	0.046	0.0069	1.646	1.32E-04
WHC-EP-0883	0-082	218-W-5	299-W7-9	24.5	0	0.3336	0.1483	0.0064	1.7084	6.30E-04
WHC-EP-0883	3-0653	VOC	299-W18-248	42.5	0	0.4223	0.1096	0.0067	1.8378	5.80E-06
WHC-EP-0883	3-0654	VOC	299-W15-216	35.6	59	0.1933	0.0186	0.0119	1.2618	2.70E-04
WHC-EP-0883	3-0657	VOC	299-W15-217	37.4	34	0.2505	0.0469	0.0145	1.3692	2.67E-04
WHC-EP-0883	4-1011	ERDF	699-35-69A	73.0	0	0.4913	0.045	0.0042	1.5218	1.00E-05

References: WHC-EP-0883, *Variability and Scaling of Hydraulic Properties for 200 Area Soils, Hanford Site.*

Khaleel et al., 1995, "Evaluation of van Genuchten-Mualem Relationships to Estimate Unsaturated Hydraulic Conductivity at Low Water Contents."

bgs = below ground surface

ERDF = Environmental Restoration Disposal Facility

VOC = volatile organic compound

Table 9. van Genuchten Parameter Values and Saturated Hydraulic Conductivities for the Six Borehole Samples Used to Represent the 200 West Area Ringold Taylor Flat Fine Unit

Data Source	Sample	Site/ Operable Unit	Borehole Number	Depth (m bgs)	Gravel Content (% wt)	θ_s (cm^3/cm^3)	θ_r (cm^3/cm^3)	α (1/cm)	n (-)	K_s (cm/s)
Khaleel et al. (1995)	0-107	218-W-5	299-W7-9	40.40	0	0.350	0.014	0.2034	1.552	2.37E-03
Khaleel et al. (1995)	0-113	218-W-5	299-W7-9	43.22	0	0.301	0.019	0.0565	1.7782	3.30E-03
PNNL-27846	B39X68	S Complex/ 216-S-13; Crib	C9513	53.38	0	0.391	0.1616	0.0051	3.831	6.99E-05
WHC-EP-0883	W7-2-94	218-W-5	299-W7-2	28.6	48	0.2168	0.0223	0.0557	1.9669	3.70E-02
WHC-EP-0883	4-0983	ERDF	699-35-69A	82.9	17	0.3373	0.010	0.0156	2.0226	5.43E-05
WHC-EP-0883	3-0655	VOC	299-W15-216	36.9	34	0.2625	0.0559	0.0029	1.6285	1.58E-04

References: WHC-EP-0883, *Variability and scaling of hydraulic properties for 200 Area soils, Hanford Site*.

Khaleel et al., 1995, "Evaluation of van Genuchten-Mualem Relationships to Estimate Unsaturated Hydraulic Conductivity at Low Water Contents."

PNNL-27846, *Physical and Hydraulic Properties of Sediments from the 200-DV-1 Operable Unit*.

bgs = below ground surface

ERDF = Environmental Restoration Disposal Facility

VOC = volatile organic compound

Table 10. Perched Water Aquifer Hydraulic Properties

Description	T (m^2/day)	K_h (m/day)	K_D[a] (K_v/K_h)	S	S_y	Test Scale[b]
Range	0.51–4.00	0.13–1.30	0.012–0.059	9.0E-04–4.5E-03	0.151–0.273	Local – intermediate
Geometric mean	2.12	0.62	0.023	2.38E-03	0.209	Local – intermediate
Arithmetic mean	2.66	0.79	0.028	2.91E-03	0.215	Local – intermediate

Source: PNNL-27846, *Physical and Hydraulic Properties of Sediments from the 200-DV-1 Operable Unit*.

a. Arbitrarily assigned K_D range for sensitivity analysis.

b. Approximate test scale length designations: local = 0.1–3 m, intermediate = 0.1–10 m, large = 0.1–>30 m.

K_h = horizontal saturated hydraulic conductivity
K_v = vertical saturated hydraulic conductivity
S = storage coefficient
S_y = specific yield
T = transmissivity

8.2 Effective Hydraulic Parameters and Variable Anisotropy

For each anisotropic EHM, the PA (Equation 3) and TCT (Equation 4) equations were used, combined with the effective retention data, to model the variable moisture-dependent macroscopic anisotropy. For the isotropic case, $p_1 = p_2 = p_3 = 0$, which corresponds to the geometric mean for $K(h)$. For the three anisotropy cases, $p_1 = p_2 = 1$ was used to determine the effective hydraulic conductivity $K_1^e(h)$ and $K_2^e(h)$ in the two horizontal directions; three different p_3 values (i.e., $p_3 = 1/3$, 0, and −1) were used to determine the effective hydraulic conductivity in the vertical direction, $K_3^e(h)$, for cases low anisotropy, intermediate anisotropy, and high anisotropy, respectively (Table 11). For all cases, identical procedures were repeated over the expected pressure head range of (−10, 0) m for various stratigraphic units. By using four different p values (i.e., 1, 1/3, 0, and −1), four sets of effective $K^e(h)$ values were obtained.

Table 11. Typical Cases with Varying Degrees of Anisotropy

Case	Anisotropy Level	*p* Value for the Horizontal Direction (i = 1, 2)	*p* Value for the Vertical Direction (i = 3)
ISO	Isotropic	0	0
LA	Low anisotropy	1	1/3
IA	Intermediate anisotropy	1	0
HA	High anisotropy	1	-1

Reference: Zhang and Khaleel, 2010, "Simulating Field-Scale Moisture Flow Using a Combined Power-Averaging and Tensorial Connectivity-Tortuosity Approach."

Note: For the Sisson and Lu field injection site in the 200 East Area (Zhang and Khaleel, 2010), the simulation results best matched the observed moisture plume behavior when the power values of 1 and 1/3 were used for determining the effective unsaturated conductivity $K^e(h)$ (h=matric potential) in the horizontal directions and vertical direction, respectively (a case of low macroscopic anisotropy).

The following steps were performed to obtain the effective parameters for moisture retention and directional unsaturated conductivity.

- Step 1: Calculate the effective moisture retention curve
- Step 2: Apply the PA model
- Step 3: Apply the TCT model

These steps are summarized below.

Step 1: Calculate the effective moisture retention curve

- For an EHM, the retention curve for the laboratory core samples between the pressure head range of (-10, 0) m (15 segments) was used to calculate the effective parameters. The pressure head range was restricted to (−10, 0) m to replicate the expected moisture regime for the CA modeling. The 15 pairs of $S^e(h)$ data constitute the effective or upscaled moisture retention curve (Equations 7 and 8) for an EHM.
  - The effective residual water content θ_r^e and the effective saturated water contents θ_s^e were obtained by simple averaging of core sample estimates
  - The effective parameters n^e and α^e were fit to the retention data.

Step 2: Apply the PA model

- For each anisotropic EHM, using the PA model (Equation 3) and an appropriate p_i (Table 11), the directional effective unsaturated hydraulic conductivity, $K_i^e(h)$ was calculated as a function of discrete pressure head, h in the i^{th} principal direction (i=1, 2, 3).

Step 3: Apply the TCT model

- Combined with the effective retention curve (step 1) for each anisotropic EHM, the Equation 3-based $K_i^e(h)$ data pairs (step 2) are described next with the TCT model, Equation 4, by fitting the effective connectivity-tortuosity coefficient L_i^e as well as the $K_i^e(h)$ data using a least-squares fit.
- The effective saturated hydraulic conductivity in the i^{th} direction, K_{si}^e, was first calculated directly using the saturated conductivity (K_s) data and used as initial estimates. The effective tortuosity-connectivity coefficient in the i^{th} direction, L_i^e as well as K_{si}^e were fitted to the $K_i^e(h)$ curve.
- For each anisotropic EHM, the preceding calculations based on steps 1 to 3 yield a total of 12 effective parameters: 4 for retention (θ_s^e, θ_r^e, α^e, and n^e) and 8 for conductivity (L_i^e, K_{si}^e; p =1, 1/3, 0, -1).

Table 12 and Table 13 list the derived effective moisture retention and the optimized PA-TCT parameters, respectively, for the HSUs in the 200 East Area. Table 14 and Table 15 list the derived effective moisture retention and the optimized PA-TCT parameters, respectively, for the HSUs in the 200 West Area.

Table 12. Effective Soil Moisture Retention Parameter Estimates for the 200 East Area Hydrostratigraphic Units

HSU	Number of Samples[a]	Data Sources	θ_s^e (cm^3/cm^3)	θ_r^e (cm^3/cm^3)	α^e (1/cm)	n^e (-)
Backfill	25	RPP-20621, PNNL-22886	0.174	0.0038	0.08859	1.271
Eolian sand	12	WHC-EP-0883	0.46708	0.04046	0.104735	1.3399
Hf1	25	RPP-20621, PNNL-22886	0.174	0.0038	0.08859	1.271
Hf2	44	RPP-20621	0.3838	0.0290	0.06419	1.6977
Hf3	25	RPP-20621, PNNL-22886	0.174	0.0038	0.08859	1.271
CCUz	11	WHC-EP-0883, Khaleel et al. (1995), PNNL-27846, WHC-EP-0645	0.3994	0.05421	0.00633	1.830

Table 12. Effective Soil Moisture Retention Parameter Estimates for the 200 East Area Hydrostratigraphic Units

HSU	Number of Samples[a]	Data Sources	θ_s^e (cm^3/cm^3)	θ_r^e (cm^3/cm^3)	α^e (1/cm)	n^e (-)
CCU sand	Sisson and Lu site unit E samples[b]	Zhang and Khaleel (2010)	0.3001	0.0393	0.04827	1.925
CCUg	25	RPP-20621, PNNL-22886	0.174	0.0038	0.08859	1.271
Rwie	25	RPP-20621, PNNL-22886	0.174	0.0038	0.08859	1.271
Ringold lower mud	11	WHC-EP-0883, Khaleel et al. (1995), PNNL-27846, WHC-EP-0645	0.3994	0.05421	0.00633	1.830
Rwia	25	RPP-20621, PNNL-22886	0.174	0.0038	0.08859	1.271

Note: Complete reference citations are provided in Chapter 11.

a. Number of samples used to represent a heterogeneous HSU as an EHM.

b. After Zhang and Khaleel, 2010. The gravel content is zero for the sediment samples that are located within the Sisson and Lu site unit E (approximately 10 to 12 m bgs) (Samples 2-1637, 2-1638, 2-2225, and 2-2234 in WHC-EP-0883).

CCU = Cold Creek unit
CCUg = Cold Creek unit gravel
CCUz = Cold Creek unit silt
Hf1 = Hanford formation unit 1
Hf2 = Hanford formation unit 2
Hf3 = Hanford formation unit 3
HSU = hydrostratigraphic unit
Rwia = Ringold Formation member of Wooded Island – unit A
Rwie = Ringold Formation member of Wooded Island – unit E

Table 13. Optimized Saturated Hydraulic Conductivity and the Pore Connectivity-Tortuosity Coefficient for Different Averaging Schemes for 200 East Area Hydrostratigraphic Units

HSU	Number of Samples*	p = 1[(a)]		p = 1/3		p = 0		p = -1	
		K_s^e (cm/s)[(b)]	L^e [(c)]	K_s^e (cm/s)	L^e	K_s^e (cm/s)	L^e	K_s^e (cm/s)	L^e
Backfill	25	4.671E-02	0.637	7.714E-03	-0.225	3.790E-03	-0.111	1.959E-04	1.471
Eolian sand	12	7.33E-03	0.2496	2.80E-03	0.7848	8.04E-04	0.9622	1.42E-05	0.0017
Hf1	25	4.671E-02	0.637	7.714E-03	-0.225	3.790E-03	-0.111	1.959E-04	1.471
Hf2	44	6.196E-03	-0.6833	6.157E-03	0.3747	6.575E-03	0.9157	7.741E-03	2.3863
Hf3	25	4.671E-02	0.637	7.714E-03	-0.225	3.790E-03	-0.111	1.959E-04	1.471
CCUz	11	2.41E-04	-1.2111	1.33E-04	0.1763	8.80E-05	1.1446	1.22E-05	1.7949
CCU sand	Sisson and Lu site unit E samples[d]	8.919E-03	-0.749	5.462E-03	0.297	4.166E-03	1.38	2.088E-03	5.67
CCUg	25	4.671E-02	0.637	7.714E-03	-0.225	3.790E-03	-0.111	1.959E-04	1.471
Rwie	25	4.671E-02	0.637	7.714E-03	-0.225	3.790E-03	-0.111	1.959E-04	1.471
Ringold lower mud	11	2.41E-04	-1.2111	1.33E-04	0.1763	8.80E-05	1.1446	1.22E-05	1.7949
Rwia	25	4.671E-02	0.637	7.714E-03	-0.225	3.790E-03	-0.111	1.959E-04	1.471

References: WHC-EP-0883, *Variability and Scaling of Hydraulic Properties for 200 Area Soils, Hanford Site*.

Zhang and Khaleel, 2010, "Simulating Field-Scale Moisture Flow Using a Combined Power-Averaging and Tensorial Connectivity-Tortuosity Approach."

*Number of samples used to represent a heterogeneous HSU as an EHM.

a. Power averaging factor (Table 11).

b. Effective saturated hydraulic conductivity.

c. Directionally dependent pore-connectivity tortuosity parameter.

d. After Zhang and Khaleel, 2010. The gravel content is zero for the sediment samples that are located within the Sisson and Lu site unit E (approximately 10 to 12 m bgs) (Samples 2-1637, 2-1638, 2-2225, and 2-2234 in WHC-EP-0883).

bgs	=	below ground surface	Hf2	=	Hanford formation unit 2
CCU	=	Cold Creek unit	Hf3	=	Hanford formation unit 3
CCUg	=	Cold Creek unit gravel	HSU	=	hydrostratigraphic unit
CCUz	=	Cold Creek unit silt	Rwia	=	Ringold Formation member of Wooded Island – unit A
EHM	=	equivalent homogeneous medium	Rwie	=	Ringold Formation member of Wooded Island – unit E
Hf1	=	Hanford formation unit 1			

Table 14. Effective Soil Moisture Retention Parameter Estimates for the 200 West Area Hydrostratigraphic Units

HSU	Number of Samples[a]	Data Sources	θ_s^e (cm^3/cm^3)	θ_r^e (cm^3/cm^3)	α^e (1/cm)	n^e (-)
Backfill	11	WCH-464, WHC-EP-0883, WHC-EP-0645	0.1917	0.0153	0.0187	1.3783
Hanford formation unit 1	11	WCH-464, WHC-EP-0883, WHC-EP-0645	0.1917	0.0153	0.0187	1.3783
Hanford formation unit 2	18[b]	WCH-464, WHC-EP-0883	0.4009	0.0428	0.0106	1.6693
Hanford formation unit 3	11	WCH-464, WHC-EP-0883, WHC-EP-0645	0.1917	0.0153	0.0187	1.3783
Cold Creek unit silt	11	WHC-EP-0883, Khaleel et al. (1995), PNNL-27846, WHC-EP-0645	0.3994	0.05421	0.00633	1.830
Cold Creek unit caliche	8	WHC-EP-0883, Khaleel et al. (1995)	0.3236	0.0639	0.007925	1.56421
Rwie	10	WHC-EP-0883	0.17056	0.01666	0.024207	1.454662
Rtf	6	PNNL-27846, Khaleel et al. (1995), WHC-EP-0883	0.3098	0.047133	0.04559	1.52301
Ringold lower mud	11	WHC-EP-0883, Khaleel et al. (1995), PNNL-27846, WHC-EP-0645	0.3994	0.05421	0.00633	1.830
Rwia	10	WHC-EP-0883	0.17056	0.01666	0.024207	1.454662

Note: Complete reference citations are provided in Chapter 11.

a. Number of samples used to represent a heterogeneous HSU as an EHM.

b. Four samples without Ks measurement were assigned the arithmetic average for power-averaging and tensorial connectivity-tortuosity model parameterization.

EHM = equivalent homogeneous medium

HSU = hydrostratigraphic unit

Rtf = Ringold Formation member of Taylor Flat

Rwia = Ringold Formation member of Wooded Island – unit A

Rwie = Ringold Formation member of Wooded Island – unit E

Table 15. Optimized Saturated Hydraulic Conductivity and the Pore Connectivity-Tortuosity Coefficient for Different Averaging Schemes for the 200 West Area Hydrostratigraphic Units

HSU	Number of Samples[a]	p = 1[b]		p = 1/3		p = 0		p = -1	
		K_s^e [c] (cm/s)	L^e [d]	K_s^e (cm/s)	L^e	K_s^e (cm/s)	L^e	K_s^e (cm/s)	L^e
Backfill	11	2.38E-03	-1.918	9.73E-04	-1.019	6.29E-04	-0.104	2.57E-04	1.7432
Hf1	11	2.38E-03	-1.918	9.73E-04	-1.019	6.29E-04	-0.104	2.57E-04	1.7432
Hf2	18	1.96E-04	-0.3724	1.56E-04	0.470	1.40E-04	1.0426	1.10E-04	2.6023
Hf3	11	2.38E-03	-1.918	9.73E-04	-1.019	6.29E-04	-0.104	2.57E-04	1.7432
CCUz	11	2.41E-04	-1.2111	1.33E-04	0.1763	8.80E-05	1.1446	1.22E-05	1.7949
CCUc	8	2.63E-04	0.6238	1.50E-04	0.6571	1.04E-04	0.6334	4.00E-05	0.6665
Rwie	10	1.15E-02	-1.8957	5.79E-03	-1.05357	3.13E-03	0.057882	4.49E-04	1.918661
Rtf	6	5.13E-03	-1.42674	3.02E-03	-0.35489	2.27E-03	0.86572	2.59E-04	1.37794
Ringold lower mud	11	2.41E-04	-1.2111	1.33E-04	0.1763	8.80E-05	1.1446	1.22E-05	1.7949
Rwie	10	1.15E-02	-1.8957	5.79E-03	-1.05357	3.13E-03	0.057882	4.49E-04	1.918661

a. Number of samples used to represent a heterogeneous HSU as an EHM.

b. Power averaging factor (Table 11).

c. Effective saturated hydraulic conductivity.

d. Directionally dependent pore-connectivity tortuosity parameter.

CCU = Cold Creek unit
CCUc = Cold Creek unit caliche
CCUz = Cold Creek unit silt
Hf2 = Hanford formation unit 2
Hf1 = Hanford formation unit 1
Hf3 = Hanford formation unit 3
EHM = equivalent homogeneous medium
HSU = hydrostratigraphic unit
Rtf = Ringold Formation member of Taylor Flat

9 Effective Transport Parameter Estimates

Base-case effective transport parameter (bulk density, diffusivity, and dispersivity) estimates are presented in this chapter. Because of natural variability, the transport parameters are all spatially variable. Similar to the flow parameters, the purpose is to evaluate the effect of such variability on the large-scale transport process.

9.1 Bulk Density

Bulk density estimates are needed to calculate the retardation factors for different species. The effective large-scale estimate for bulk density is the average of the small-scale laboratory measurements for bulk density (Gelhar, 1993). Table 16 and Table 17 provide the effective, large-scale bulk density estimates for the HSUs in the 200 East and 200 West Areas, respectively.

Table 16. Bulk Density Estimates for the 200 East Area Hydrostratigraphic Units

Hydrostratigraphic Unit	Range (g/cm^3)	Average Bulk Density (g/cm^3)
Backfill[a,b]	1.89 - 2.38	2.15
Eolian sand[d]	1.51 - 1.98	1.67
Hanford formation unit 1[a,b]	1.89 - 2.38	2.15
Hanford formation unit 2[a]	1.51 - 1.98	1.67
Hanford formation unit 3[a,b]	1.89 - 2.38	2.15
Cold Creek unit silt [c,d,e,f]	1.43 - 1.75	1.59
Cold Creek unit sand[e]	1.60 - 1.75	1.66
Cold Creek unit gravel [a,b]	1.89 - 2.38	2.15
Ringold Formation member of Wooded Island – unit E[a,b]	1.89 - 2.38	2.15
Ringold lower mud[c,d,e,f]	1.43 - 1.75	1.59
Ringold Formation member of Wooded Island – unit A[a,b]	1.89 - 2.38	2.15

a. RPP-20621, *Far-Field Hydrology Data Package for the Integrated Disposal Facility Performance Assessment.*

b. PNNL-22886, *System-Scale Model of Aquifer, Vadose Zone, and River Interactions for the Hanford 300 Area – Application to Uranium Reactive Transport*.

c. WHC-EP-0645, *Performance Assessment for the Disposal of Low-Level Waste in the 200 West Area Burial Grounds*.

d. WHC-EP-0883, *Variability and Scaling of Hydraulic Properties for 200 Area Soils, Hanford Site.*

e. Khaleel et al., 1995, "Evaluation of van Genuchten-Mualem Relationships to Estimate Unsaturated Hydraulic Conductivity at Low Water Contents."

f. PNNL-27846, *Physical and Hydraulic Properties of Sediments from the 200-DV-1 Operable Unit*.

Table 17. Bulk Density Estimates for the 200 West Area Hydrostratigraphic Units

Hydrostratigraphic Unit	Range (g/cm^3)	Average Bulk Density (g/cm^3)
Backfill[a,b,c]	1.85 - 2.19	2.03
Hanford formation unit 1[a,b,c]	1.85 – 2.19	2.03
Hanford formation unit 2[a,c]	1.40 - 1.98	1.70
Hanford formation unit 3[a,b,c]	1.85 – 2.19	2.03
Cold Creek unit silt [b,c,d,e]	1.43 - 1.75	1.59

Table 17. Bulk Density Estimates for the 200 West Area Hydrostratigraphic Units

Hydrostratigraphic Unit	Range (g/cm^3)	Average Bulk Density (g/cm^3)
Cold Creek unit caliche[c,d]	1.34 - 1.83	1.55
Ringold Formation member of Wooded Island – unit E[c]	1.93 - 2.32	2.13
Ringold Formation member of Taylor Flat [c,d,e]	1.63 - 1.94	1.70
Ringold lower mud [b,c,d,e]	1.43 - 1.75	1.59
Ringold Formation member of Wooded Island – unit A[c]	1.93 - 2.32	2.13

a. WCH-464, *Hydrologic Data Package in Support of Environmental Restoration Disposal Facility Performance Assessment Modeling*.

b. WHC-EP-0645, *Performance Assessment for the Disposal of Low-Level Waste in the 200 West Area Burial Grounds*.

c. WHC-EP-0883, *Variability and scaling of hydraulic properties for 200 Area soils, Hanford Site*.

d. Khaleel et al. (1995), "Evaluation of van Genuchten-Mualem Relationships to Estimate Unsaturated Hydraulic Conductivity at Low Water Contents."

e. PNNL-27846, *Physical and Hydraulic Properties of Sediments from the 200-DV-1 Operable Unit*.

9.2 Diffusivity

It is assumed that the effective, large-scale diffusion coefficients for all HSUs are a function of volumetric moisture content, θ and can be estimated based on an empirical relation (Millington and Quirk, 1961, "Permeability of Porous Solids"):

$$D_e(\theta) = D_0 \frac{\theta^{10/3}}{\theta_s^2} \qquad \text{(Eq. 9)}$$

where: $D_e(\theta)$ is the effective diffusion coefficient of an ionic species and D_0 is the effective diffusion coefficient for the same species in free water. The molecular diffusion coefficient for all species in pore water is assumed to be 2.5×10^{-5} cm^2/sec (WHC-SD-WM-EE-004, *Performance Assessment of Grouted Double-Shell Tank Waste Disposal at Hanford*).

9.3 Vadose Zone Macrodispersivities

Field-scale dispersivities are referred to as macrodispersivities. The terms macrodispersivity and dispersivity are used interchangeably in this section. Details on how the selections are made using different methods are provided in Appendix B of RPP-ENV-58782, *Performance Assessment of Waste Management Area C, Hanford Site, Washington*.

Field observations indicate that the dispersion coefficients required to describe the large-scale transport processes, at field scales of tens or hundreds of meters, are much different from those observed in small-scale laboratory experiments (Gelhar, 1993). In fact, field-scale dispersivities may often be orders of magnitude larger than those observed in the laboratory. Consequently, laboratory-scale dispersivities, which are typically approximately 1 cm or less, are of little use in estimating field-scale dispersivities.

There is general agreement in hydrology literature that hydraulic conductivity variations induced by field-scale heterogeneities play an important role in field-scale transport processes. However, there does not appear to be a clear consensus about how best to describe such processes quantitatively (Gelhar, 1993). While well-designed, large-scale tracer experiments would provide useful information, limited field data are available at this time to quantify macrodispersivities in unsaturated media.

Dispersivities are a function of matric potential (or soil moisture content) in unsaturated media (Mantoglou and Gelhar, 1987, "Stochastic Modeling of Large-Scale Transient Unsaturated Flow Systems"; Russo, 1991, "Stochastic Analysis of Simulated Vadose Zone Solute Transport in a Vertical Cross Section of Heterogeneous Soil During Nonsteady Water Flow"; Russo, 1993, "Stochastic Modeling of Macrodispersion for Solute Transport in a Heterogeneous Unsaturated Porous Formation"). As with saturated media, heterogeneities that exist at various length scales result also in a scale dependence of macrodispersivities in unsaturated media (Gelhar et al., 1992, "A Critical Review of Data on Field-Scale Dispersion in Aquifers"). Dispersivities increase with time, or equivalently with distance, until they tend to converge on their unique asymptotic (large-time) values. However, it can take a long time (e.g., years or decades) for the asymptotic Fickian approximation to take hold. The well-known asymptotic behavior is usually attributed to heterogeneity-induced spreading and mixing until the point at which the heterogeneity has effectively been "sampled" by the contaminant plume such that dispersion becomes constant. As with other numerical simulation work, the use of a constant (asymptotic) macrodispersivity for CA modeling is considered appropriate (NUREG/CR-6114, *Auxiliary Analyses in Support of Performance Assessment of a Hypothetical Low-Level Waste Facility: Groundwater Flow and Transport Simulation*; NUREG/CR-5965, *Modeling Field Scale Unsaturated Flow and Transport Processes*). The second-moment evolution or the time-dependent, preasymptotic dispersivities are of marginal interest in simulations involving long times or large-mean travel distances such as those for CA modeling.

Note that because of the relatively dry moisture regime, unsaturated media macrodispersivity estimates are expected to be smaller, compared to saturated media estimates. Also note that unlike saturated media, the vadose zone flow is typically perpendicular to geologic bedding. Numerical simulations of vadose zone transport for Hf2 sands demonstrated that the longitudinal macrodispersivities for flow perpendicular to bedding are smaller than those for flow parallel to bedding (Khaleel et al., 2002, "Upscaled Flow and Transport Properties for Heterogeneous Unsaturated Media"). For both perpendicular and parallel to bedding, macrodispersivities increase as the mean matric potential becomes more negative. However, the Fickian regime is reached much earlier for cases with flow perpendicular to bedding than for parallel to bedding (Khaleel et al., 2002).

A range of estimates on the basis of numerical simulations, stochastic theory, and experimental observations is provided in Section 9.4. To obtain macrodispersivity, the local pore-scale dispersivities, which are typically small (<1 cm), are not included either in numerical simulations or stochastic solutions. This is consistent with the approach used by other investigators (Yang et al., 1997, "Stochastic analysis of adsorbing solute transport in three-dimensional, heterogeneous, unsaturated soils"; Gelhar, 1993; Gelhar and Axness, 1983, "Three-Dimensional Stochastic Analysis of Macrodispersion in Aquifers").

9.4 Estimated Macrodispersivities

Table 18 summarizes the macrodispersivity estimates based on results of numerical simulation, stochastic theory, and the 200 Areas experimental data. Overall, the recommended asymptotic macrodispersivity estimates are consistent with values reported in literature for relatively dry unsaturated media (e.g., Figure 10).

For the sandy media, estimates are available by all three methods: numerical simulation, stochastic solutions, and field experiments. However, for the CA modeling (for the sandy units), the recommendation is to use longitudinal macrodispersivity values ranging from 25 cm (based on numerical simulations [Khaleel et al., 2002]) to 100 cm (based on field experiments [Appendix E in RPP-20621]). The 100 cm estimate is based on extrapolation of field data up to a length scale of 10 m (Figure 10).

Table 18. Longitudinal Macrodispersivity Estimates and Ranges for the Hydrostratigraphic Units

Hydrostratigraphic Unit	Recommended Macrodispersivity Estimate (cm)	Approximate Estimated ranges (cm)
Sand-dominated units* (Eolian sand, Hanford formation unit 2, Ringold Formation member of Taylor Flat, Cold Creek unit sand)	25	25 – 100
Gravel-dominated units* (Backfill, Hanford formation units 1 and 3, Cold Creek unit gravel, Ringold Formation member of Wooded Island – units E and A)	15	15 – 30
Fine-textured units* (Cold Creek unit silt, Cold Creek unit caliche, Ringold lower mud)	5	5 – 10

*Source: Appendix B in RPP-ENV-58782, *Performance Assessment of Waste Management Area C, Hanford Site, Washington*.

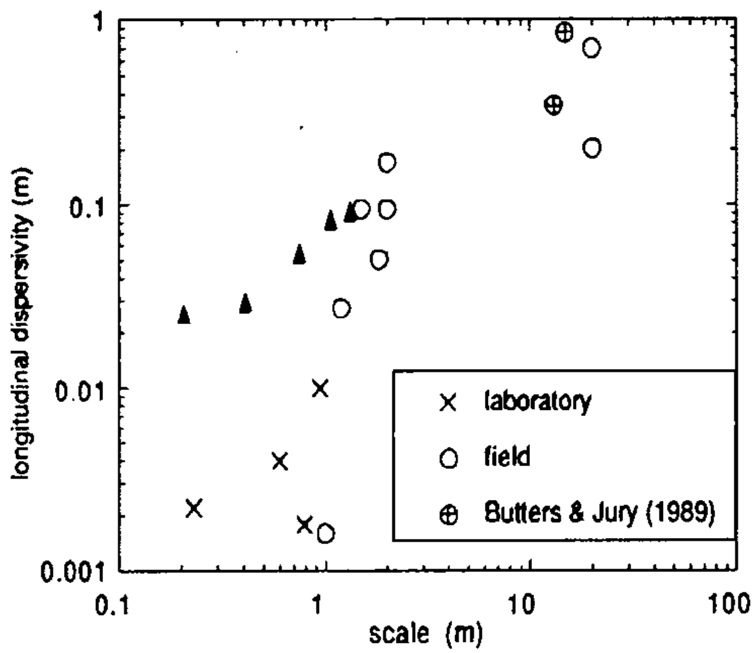

Note: The triangles are data from Appendix E of RPP-20621, *Far-Field Hydrology Data Package for the Integrated Disposal Facility Performance Assessment*.

References: Butters and Jury, 1989, "Field Scale Transport of Bromide in an Unsaturated Soil; Dispersion Modeling."
Gelhar, 1993, "Stochastic Subsurface Hydrology."

Figure 10. Longitudinal Laboratory- and Field-Scale Dispersivities in Unsaturated Media as a Function of Overall Problem Scale

The perturbation analysis for the stochastic solutions applies to small variance estimates. As reported in Appendix B in RPP-ENV-58782, because of the large variance of unsaturated hydraulic conductivity estimate ($\sigma^2_{LnK_u}$) for the sandy media, stochastic theory-based estimates are often considerably larger than those based on numerical simulations and field experiments, and are not included in Table 18. However, the preceding estimates for sandy sediments compare well with those reported elsewhere (e.g., PNNL-25146, *Scale-Dependent Solute Dispersion in Variably Saturated Porous Media*). Using different methods, PNNL-25146 notes that the longitudinal dispersivity estimates for the 200 Areas sandy sediments can range from tens of centimeters to as high as 100 cm.

Unlike the sandy media, the calculated variance ($\sigma^2_{LnK_u}$) for the gravelly and silty units are much lower. For the gravelly media, as reported in Appendix B in RPP-ENV-58782, the recommendation is to use, based on stochastic theory, longitudinal macrodispersivity values ranging from 15 to 30 cm (Table 18). This is again consistent with the estimates (i.e., 15 to 43 cm), based on other methods, for the 200 Areas gravelly media (PNNL-25146). The contrast in $\sigma^2_{LnK_u}$ estimates for the Hanford Site sandy and gravelly media is illustrated in Figure 11; the observed log unsaturated conductivity variance for the gravelly sediments is much lower than that for the sandy sediments. Consequently, the calculated dispersivities for the gravelly sediments are expected to be lower than those for the sandy sediments Table 18).

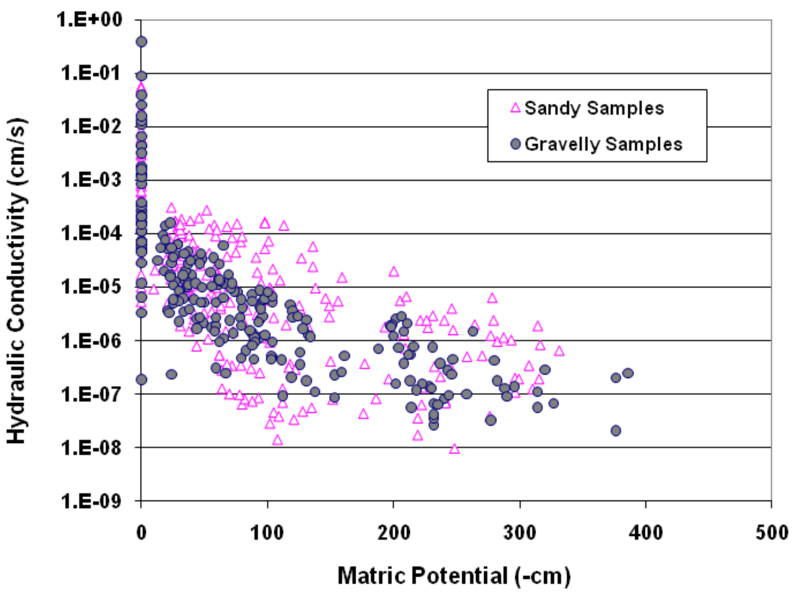

Source: Khaleel and Relyea, 2001, "Variability of Gardner's α for Coarse-Textured Sediments."

Figure 11. Unsaturated Hydraulic Conductivity Measurements for Sand- and Gravel-Dominated Samples

For the fine-textured units, the recommendation is to use, based on stochastic theory, longitudinal macrodispersivity values ranging from 5 to 10 cm (Table 18). Overall, the sequence of magnitudes for macrodispersivities follows the sequence of reduction in variance for the sandy, gravelly, and fine-textured sediments. The asymptotic macrodispersivity estimates in Table 18 are for a relatively dry moisture regime (i.e., $\sigma^2_{LnK_u}$ estimated for mean tensions of 2 m for the sandy units, 3 to 4 m for the gravelly units, and 1 to 2 m for the silty units).

The transverse macrodispersivity is typically much lower; in saturated media, it typically ranges from 1% to 10% of the longitudinal macrodispersivity (Gelhar and Axness, 1983). In the absence of unsaturated media experimental data, the recommendation is to use a transverse macrodispersivity 1/10th of the longitudinal macrodispersivity (PNNL-23711, PNNL-25146).

10 Summary

For the CA subsurface flow and transport analyses, an EHM modeling approach will be used to represent the heterogeneous Hanford Site sediments. Following the EHM modeling approach, small-scale core measurements are used to predict the large, field-scale flow behavior. The existing database on sediment physical and hydraulic properties for the broader 200 Areas was queried for information regarding sediment PSD, soil moisture retention, saturated as well as unsaturated hydraulic conductivity. The following three-step process was used to develop the hydraulic properties and transport parameters for the CA modeling.

1. **Breakdown** of existing database on hydraulic properties by HSUs
2. **Constitutive model** parameters for laboratory, core-scale hydraulic properties
3. **Upscaling** for macroscopic, field-scale flow, and transport parameters

The breakdown of hydraulic properties for the 200 Areas sediments by HSUs was done as follows:

- Based on the available ROCSAN database and distinct differences in PSD for the 200 East and 200 West Area sediments, the database was partitioned, and the hydraulic properties database developed separately for the two areas.
- The properties for the HSUs are categorized as three combined grouping of units (i.e., sand-dominated, gravel-dominated, and fine-textured units) based on the ROCSAN database and the PSD of the sediment samples.
- Sand-dominated units include: Eolian sand, Hf2, Cold Creek unit sand, and Rtf.
- Gravel-dominated units include: Backfill, Hf1, Hf3, CCUg, Rwie, and Rwia.
- Fine-textured units include: CCUz, CCUc, and Ringold lower mud (silt and clay).

The criteria and database for development of constitutive model parameters for core-scale hydraulic properties are as follows:

- The laboratory database for core samples is based on published reports (i.e., RPP-20621; PNNL-23711; PNNL-22886, *System-Scale Model of Aquifer, Vadose Zone, and River Interactions for the Hanford 300 Area – Application to Uranium Reactive Transport*; PNNL-27846; WHC-EP-0883; WHC-EP-0645, *Performance Assessment for the Disposal of Low-Level Waste in the 200 West Area Burial Grounds*; Khaleel et al., 1995, "Evaluation of van Genuchten-Mualem Relationships to Estimate Unsaturated Hydraulic Conductivity at Low Water Contents"; Zhang and Khaleel, 2010).
- Bulk of the sediment samples include data on PSD, saturated hydraulic conductivity, moisture retention and unsaturated hydraulic conductivity.
- For majority of samples, a simultaneous fit of moisture retention, and saturated and unsaturated hydraulic conductivity data were used to derive the constitutive model (van Genuchten-Mualem) parameters for core samples.

Upscaling for macroscopic, field-scale flow, and transport parameters was accomplished as follows:

- The vadose zone heterogeneous geologic media was conceptualized as being comprised of multiple EHMs.
- Each heterogeneous HSU is treated as an anisotropic EHM having its individual upscaled (effective) flow and transport properties.
- Upscaled flow properties and the macroscopic anisotropy for the field scale are based on a variable MDA model.
- Macrodispersivity estimates for various HSUs are based on a combination of numerical simulation results, stochastic solutions, and the 200 East Area tracer experiments.

An overall assessment of upscaled hydraulic properties suggests that the distinct differences in PSD data for the two areas are reflected in the hydraulic properties for the 200 East and 200 West Area sediments. For example, as expected, the moisture holding capacity for the effective (upscaled) retention curve is higher for the 200 West Area Hanford Hf2 sediments compared with the effective retention curve for the 200 East Area Hanford Hf2 sediments. The optimized saturated hydraulic conductivities for the 200 West Area Hanford Hf2 sediments are smaller than those for the 200 East Area Hf2 sediments. The field-scale macroscopic anisotropy is larger for the sand-dominated Hf2 sediments than for the gravel-dominated Hf1/Hf3 sediments. The air-entry pressure heads for the fine-textured CCUz and CCUc sediments are considerably larger than those for the sand- and gravel-dominated sediments. The optimized saturated hydraulic conductivities for the CCUz and CCUc sediments are smaller than those for the sand- and gravel-dominated sediments in the 200 East and 200 West Areas.

Based on the documented field-testing results for Hanford Site sediments (Zhang and Khaleel, 2010), the low anisotropy case (p =1 for the x- and y-directions and p =1/3 for the z-direction) is the recommendation for the CA flow simulations. For the S&L field injection site in the 200 East Area, the simulation results best matched the observed moisture plume behavior when the power values of 1 and 1/3 were used for determining the effective unsaturated conductivity $K^e(h)$ [h=matric potential] in the horizontal and vertical directions, respectively (i.e., a case of low macroscopic anisotropy).

A PWA region exists in B Complex in the 200 East Area. Based on analysis of slug test results, the report includes the hydraulic properties for the PWA.

11 References

Ababou, R., 1996, “Random Porous Media Flow on Large 3-D Grids: Numerics, Performance, and Application to Homogenization,” *Environmental Studies*, M.F. Wheeler (ed.), Springer-Verlag, New York, New York, pp. 1–25.

Burdine, N.T., 1953, “Relative Permeability Calculations from Pore-Size Distribution Data,” *Journal of Petroleum Technology* 5(3).

Butters, G.L., and W.A. Jury, 1989, “Field Scale Transport of Bromide in an Unsaturated Soil: 2. Dispersion Modeling,” *Water Resources Research* 25(7):1583–1589.

Dagan, G.,1989, *Flow and Transport in Porous Formations*, Springer-Verlag, Berlin, Germany.

Gelhar, L.W., 1993, *Stochastic Subsurface Hydrology*, Prentice Hall, New York, New York.

Gelhar, L.W. and C.L. Axness, 1983, “Three-Dimensional Stochastic Analysis of Macrodispersion in Aquifers,” *Water Resources Research* 19(1):161–180.

Gelhar, L.W., C. Welty, and K.R. Rehfeldt, 1992, "A Critical Review of Data on Field-Scale Dispersion in Aquifers," *Water Resources Research* 28(7):1955–1974.

Green, T.R., J.E. Constantz, and D.L. Freyberg, 1996, "Upscaled Soil-Water Retention Using van Genuchten's Function," *Journal of Hydrologic Engineering* 1(3):123–130.

Khaleel, R. and J. F. Relyea, 2001, "Variability of Gardner's α for Coarse-Textured Sediments," *Water Resources Research* 37(6):1567–1575.

Khaleel, R., J. F. Relyea, and J. L. Conca, 1995, "Evaluation of van Genuchten-Mualem Relationships to Estimate Unsaturated Hydraulic Conductivity at Low Water Contents," *Water Resources Research* 31(11):2659–2668.

Khaleel, R., T.C.J. Yeh, and Z. Lu, 2002, "Upscaled Flow and Transport Properties for Heterogeneous Unsaturated Media," *Water Resources Research* 38(5):11-1–11-12.

Mantoglou, A. and L.W. Gelhar, 1987, "Stochastic Modeling of Large-Scale Transient Unsaturated Flow Systems," *Water Resources Research* 23(1):37–46.

Matheron, G.,1967, *Eléments pour une Théorie des Milieux Poreux*, Masson, Paris.

Millington, R.J. and J.P. Quirk, 1961, "Permeability of Porous Solids," *Transactions of the Faraday Society* 57:1200–1207.

Mualem, Y., 1976, "A New Model for Predicting the Hydraulic Conductivity of Unsaturated Porous Media," *Water Resources Research* 12(3):513–522.

National Research Council, 2001, *Science and Technology for Environmental Cleanup at Hanford*, National Research Council, National Academy Press, Washington, D.C.

NUREG/CR-5965, 1994, *Modeling Field Scale Unsaturated Flow and Transport Processes*, Department of Civil and Environmental Engineering, Massachusetts Institute of Technology, Cambridge, Massachusetts. Available at: https://www.osti.gov/biblio/10182911.

NUREG/CR-6114, 1994, *Auxiliary Analyses in Support of Performance Assessment of a Hypothetical Low-Level Waste Facility: Groundwater Flow and Transport Simulation*, Vol. 3, Department of Civil and Environmental Engineering, Massachusetts Institute of Technology, Cambridge, Massachusetts. Available at: https://www.osti.gov/biblio/145213.

PNNL-12030, 2000, *STOMP Subsurface Transport Over Multiple Phases Version 2.0 Theory Guide*, Pacific Northwest National Laboratory, Richland, Washington. Available at: https://stomp.pnl.gov/documentation/theory.pdf.

PNNL-19277, 2010, *Conceptual Models for Migration of Key Groundwater Contaminants Through the Vadose Zone and Into the Unconfined Aquifer Below the B-Complex*, Pacific Northwest National Laboratory, Richland, Washington. Available at: https://pdw.hanford.gov/document/0084238.

PNNL-22886, 2013, *System-Scale Model of Aquifer, Vadose Zone, and River Interactions for the Hanford 300 Area – Application to Uranium Reactive Transport*, RPT-DVZ-AFRI-019, Pacific Northwest National Laboratory, Richland, Washington. Available at: https://www.pnnl.gov/main/publications/external/technical_reports/PNNL-22886.pdf.

PNNL-23711, 2015, *Physical, Hydraulic, and Transport Properties of Sediments and Engineered Materials Associated with Hanford Immobilized Low-Activity Waste*, RPT-IGTP-004, Rev. 0, Pacific Northwest National Laboratory, Richland, Washington. Available at: https://www.pnnl.gov/main/publications/external/technical_reports/PNNL-23711.pdf.

PNNL-25146, 2016, *Scale-Dependent Solute Dispersion in Variably Saturated Porous Media*, RPT-IGTP-009, Rev. 0, Pacific Northwest National Laboratory, Richland, Washington. Available at: https://www.pnnl.gov/main/publications/external/technical_reports/PNNL-25146.pdf.

PNNL-27846, 2018, *Physical and Hydraulic Properties of Sediments from the 200-DV-1 Operable Unit*, RPT-DVZ-CHPRC 0005, Rev. 0, Pacific Northwest National Laboratory, Richland, Washington. Available at: https://www.osti.gov/biblio/1468972.

Polmann, D.J., 1990, "Application of Stochastic Methods to Transient Flow and Transport in Heterogeneous Unsaturated Soils," Ph.D. Thesis, Department of Civil Engineering, Massachusetts Institute of Technology, Cambridge, Massachusetts.

Raats, P.A.C., Z.F. Zhang, A.L. Ward, and G.W. Gee, 2004, "The Relative Connectivity-Tortuosity Tensor for Conduction of Water in Anisotropic Unsaturated Soils," *Vadose Zone Journal* 3(3):1471–1478.

RPP-20621, 2004, *Far-Field Hydrology Data Package for the Integrated Disposal Facility Performance Assessment*, Rev. 0, CH2M HILL Hanford Group, Inc., Richland, Washington. Available at: https://pdw.hanford.gov/document/0064586H.

RPP-ENV-58782, 2016, *Performance Assessment of Waste Management Area C, Hanford Site, Washington*, Rev. 0, Washington River Protection Solutions, Richland, Washington. Available at: https://pdw.hanford.gov/document/0072363H.

Russo, D., 1991, "Stochastic Analysis of Simulated Vadose Zone Solute Transport in a Vertical Cross Section of Heterogeneous Soil During Nonsteady Water Flow," *Water Resources Research* 27(3):267–283.

Russo, D., 1993, "Stochastic Modeling of Macrodispersion for Solute Transport in a Heterogeneous Unsaturated Porous Formation," *Water Resources Research* 29(2):383–397.

van Genuchten, M. Th., 1980, "A Closed-Form Equation for Predicting the Hydraulic Conductivity of Unsaturated Soils," *Soil Science Society of America Journal* 44(5):892–898.

WCH-464, 2013, *Hydrologic Data Package in Support of Environmental Restoration Disposal Facility Performance Assessment Modeling*, Rev. 0, Washington Closure Hanford, Richland, Washington.

WHC-EP-0645, 1995, *Performance Assessment for the Disposal of Low-Level Waste in the 200 West Area Burial Grounds*, Westinghouse Hanford Company, Richland, Washington. Available at: https://pdw.hanford.gov/document/0075582H.

WHC-EP-0883, 1995, *Variability and Scaling of Hydraulic Properties for 200 Area Soils, Hanford Site*, Westinghouse Hanford Company, Richland, Washington. Available at: https://www.osti.gov/servlets/purl/188564.

WHC-SD-WM-EE-004, 1995, *Performance Assessment of Grouted Double-Shell Tank Waste Disposal at Hanford*, Rev. 1, Westinghouse Hanford Company, Richland, Washington.

Yang, J., R. Zhang, J. Wu, and M. B. Allen, 1997, "Stochastic Analysis of Adsorbing Solute Transport in Three-Dimensional, Heterogeneous, Unsaturated Soils," *Water Resources Research* 33(3):1947–1956.

Ye, M., R. Khaleel, and T.-C.J. Yeh, 2005, "Stochastic Analysis of Moisture Plume Dynamics of a Field Injection Experiment," *Water Resources Research* 41, W03013.

Yeh, T.C.J., L.W. Gelhar and A.L. Gutjahr, 1985, "Stochastic Analysis of Unsaturated Flow in Heterogeneous Soils, 2. Statistically Anisotropic Media with Variable α," *Water Resources Research* 21(4):457–464.

Yeh, T.-C.J. Yeh, M. Ye, and R. Khaleel, 2005, "Estimation of Effective Unsaturated Hydraulic Conductivity Tensor Using Spatial Moments of Observed Moisture Plume," *Water Resources Research* 41, W03014.

Yeh, T.C.J., R. Khaleel, and K.C. Carroll, 2015, *Flow Through Heterogeneous Geologic Media*, Cambridge University Press, New York.

Zhang, Z.F., A.L. Ward, and G.W. Gee, 2003, "A Tensorial Connectivity–Tortuosity Concept to Describe the Unsaturated Hydraulic Properties of Anisotropic Soils," *Vadose Zone Journal* 2(3):313–321.

Zhang, Z.F., and R. Khaleel, 2010, "Simulating Field-Scale Moisture Flow Using a Combined Power-Averaging and Tensorial Connectivity-Tortuosity Approach," *Water Resources Research* 46, W09505.